Mathematical models: a key to understanding HIV envelope interactions?

Magnus, Carsten ; Brandenberg, Oliver F ; Rusert, Peter ; Trkola, Alexandra ; Regoes, Roland Robert

Abstract: The spikes of the human immunodeficiency virus (HIV) mediate viral entry and are the most important targets for neutralizing antibodies. Each spike consists of three identical subunits. The role of the spike's subunits in antibody binding is not fully understood. One experimental approach to analyze trimer function uses assays with mixed envelope trimer expressing cells or viruses. As these experiments do not allow direct observation of subunit functions, mathematical models are required to interpret them. Here we describe a modeling framework to study (i) the interaction of the V1V2 loop with epitopes on the V3 loop and (ii) the composition of quaternary epitopes. In a first step we identify which trimers can form in these assays and how they function under antibody binding. We then derive the behavior of an average trimer. We contrast two experimental reporting systems and list their advantages and disadvantages. In these experiments trimer formation might not be perfectly random and we show how these effects can be tested. As we still lack a potent vaccine against HIV, and this vaccine surely has to stimulate the production of neutralizing antibodies, mixed trimer approaches in combination with mathematical models will help to identify vulnerable sites of the HIV spike.

DOI: https://doi.org/10.1016/j.jim.2013.09.002

Mathematical models: a key to understanding HIV envelope interactions?

Carsten Magnus[a,*], Oliver F. Brandenberg[a], Peter Rusert[a], Alexandra Trkola[a], Roland R. Regoes[b]

[a] *Institute of Medical Virology, University of Zurich, Switzerland*
[b] *Integrative Biology, ETH Zurich, Switzerland*

Abstract

The spikes of the human immunodeficiency virus (HIV) mediate viral entry and are the most important targets for neutralizing antibodies. Each spike consists of three identical subunits. The role of the spike's subunits in antibody binding is not fully understood. One experimental approach to analyze trimer function are assays with mixed envelope trimer expressing cells or viruses. As these experiments do not allow direct observation of subunit functions, mathematical models are required to interpret them. Here we describe a modeling framework to study (i) the interaction of the V1V2 loop with epitopes on the V3 loop and (ii) the composition of quaternary epitopes. In a first step we identify which trimers can form in these assays and how they function under antibody binding. We then derive the behavior of an average trimer. We contrast two experimental reporting systems and list their advantages and disadvantages. In these experiments trimer formation might not be perfectly random and we show how these effects can be tested.

*corresponding author
Email address: magnus.carsten@virology.uzh.ch (Carsten Magnus)

As we still lack a potent vaccine against HIV, and this vaccine surely has to stimulate the production of neutralizing antibodies, mixed trimer approaches in combination with mathematical models will help to identify vulnerable sites of the HIV spike.

Keywords: human immunodeficiency virus envelope interactions, epitope masking by variable loops 1 and 2, quaternary epitopes, mathematical models

---

1. Introduction

HIV-1 enters target cells by virtue of its envelope glycoprotein spikes incorporated into the viral membrane [17, 80]. Envelope glycoproteins (Env) form heterodimers (in structural context referred to as *protomer*), comprising a gp120 subunit non-covalently linked to the transmembrane subunit gp41 and assemble as trimers to form the functional spike [59, 75, 84]. Binding of envelope-specific antibodies to the envelope trimer interferes with the entry process and results in virus neutralization [4, 35]. Eliciting neutralizing antibodies to HIV is considered a crucial function of an effective HIV vaccine [3, 23, 48, 71]. However, despite a vigorous antibody response directed to the HIV envelope proteins, potent and broadly neutralizing antibodies are scarce [15]. A number of factors account for this, foremost the architecture of the viral envelope spike, which restricts binding of antibodies to vulnerable sites on the envelope trimer. The trimeric arrangement of the protomers, an extensive and variable glycan shield, protection of receptor-binding sites by conformational masking, and variable loops that shield distant epitopes within the trimer all act in synergy to protect the envelope proteins from

antibody attack [5, 8, 34, 36, 45, 62, 65, 77, 82].

The variable loops 1 and 2 (V1V2) play a dominant role in shielding the envelope trimer against neutralizing antibodies [6, 32, 51, 55, 66, 83]. A marked increase in sensitivity to antibodies directed against the V3 loop, the CD4-binding site and CD4-induced epitopes can be observed upon the introduction of certain mutations within V1V2, or upon deletion of the entire V1V2 domain [7, 16, 26, 38, 41, 42, 52, 56, 63, 68, 70, 81, 90]. V1V2 also appears to be involved in the entry process [6, 20, 30, 31, 53, 54, 61, 69, 72–74, 85]. During the course of the infection, HIV undergoes a substantial sequence evolution within each infected individual. Over time the evolving viral quasipecies portray a high sequence variability in the V1V2 domain, including length polymorphisms and variable glycosylation patterns, likely reflecting both direct antibody pressure on V1V2 as well as the need to adapt its shielding to antibodies directed against distal epitopes [1, 9, 10, 14, 18, 21, 25, 37, 39, 58, 63]. A similar effect has been reported on the population level, where the length and number of glycosylation sites of V1V2 have been suggested to have increased over the course of the HIV-1 pandemic [2, 11].

To date, no crystal structure of the V1V2 domain in the context of gp120 has been obtained, thus detailed, atomic level information of the structure and position of the V1V2 domain in the context of a single gp120 subunit both in the monomeric state and in the assembled trimer are missing [33]. Cryo-electron microscopy (cryo-EM) studies provide strong evidence that V1V2 resides at the apex of the spike, where it interacts with the V3 loop [24, 39, 47, 79]. Recent studies reported a structure of the spike at high resolution, allowing the discrimination of individual domains within gp120,

and identified the interaction between V1V2 and V3 at the spike apex as the major trimer association domain between individual gp120 subunits [46, 47].

In recent years, cryo-EM reconstructions have proven valuable in studying and understanding global interactions between Env trimers and neutralizing antibodies. However, these techniques do not provide atomic level resolution and therefore cannot resolve functional details on the HIV entry process nor on the modes of trimer interaction with antibodies. One experimental approach that has proven useful in studying such complex processes and interactions is based on the production and analysis of mixed envelope trimers, i.e. trimers consisting of envelope subunits which differ in sequence and functionality. Mixed trimers are generated by co-transfection of suitable cells with the respective envelope encoding plasmids, resulting in either cells or pseudotyped virions displaying mixed trimers on their surface. These mixed trimer expressing cells or virions can be utilized in antibody binding studies, neutralization or entry assays. Complicated stochastic effects during trimer formation and expression as well as during entry, antibody binding and neutralization makes it necessary to analyze the resulting data with mathematical models as we previously demonstrated [43–45, 62]. Mixed trimer approaches have been used to study the stoichiometries of the HIV entry process, namely the number of trimers needed for entry [28, 45, 87] (*stoichiometry of entry*, denoted by T), the number of antibodies needed to neutralize a trimer [28, 43, 67, 86] (*stoichiometry of trimer neutralization*, denoted by N) , the number of required functional subunits within a trimer [44, 88] (*subunit stoichiometry*, denoted by S or σ), the effect of complementation between protomers within the trimer [64], and the formation of

quaternary epitopes [76].

We recently utilized a mixed trimer approach to define the interaction between V1V2 and V3 with the aim to unravel the molecular basis for the potent shielding of V3 by V1V2 [62]. Two different mechanisms can be envisioned in this context: (i) The V1V2 loop of a given gp120 protomer within a trimer interacts with the V3 loop on a neighboring gp120 subunit, and thereby shields epitopes located on the neighboring V3 loop from antibody binding. This inter-protomeric mode of shielding is referred to as *neighboring or trans protection*. (ii) The V1V2 interacts with the V3 loop that belongs to the same gp120 subunit. This intra-protomeric mode of shielding is referred to as *self or cis protection* (see Figure 1 A). By studying antibody binding to the mixed trimers expressed on cells with flow cytometry and following analysis with mathematical models, we concluded inter-protomeric (i.e. neighboring or trans) shielding of the V3 loop by the V1V2 domain. However, another study, employing a mixed trimer approach based on an infectivity readout without detailed mathematical analysis, came to the opposite conclusion, namely intra-protomeric (i.e. self or cis) interaction of V1V2 with the V3 loop [40]. Based on our current understanding both observations could potentially be correct. This might be the case if the V1V2 can adopt more than one conformation on the intact trimer or if the V1V2 conformation is strain dependent. Further, based on the trimer structure described by Mao et al. [46, 47] it remains possible that the V1V2 domains contacts V3 loops both from its own and a neighboring subunit at the spike apex.

The interaction between V1V2 and V3 is of relevance not only for antibody shielding, but it also constitutes epitopes that can be recognized by

neutralizing antibodies. In many cases these epitopes appear to be preferentially formed on intact trimers and not on soluble gp120 molecules and are referred to as *quaternary epitopes*. Several antibodies recognizing quaternary epitopes depending on both V1V2 and V3 have been isolated, including the broad and potent antibodies PG9 and PG16 [19, 60, 76]. Recently, co-crystal structures of the V1V2 loop with PG9 were used to identify interaction sites in this complex at an atomic level [49]. However, this approach does not clarify why theses antibodies preferentially bind to trimers and not to monomeric gp120. [27] combined electron microscopy, small angle X-ray scattering, size exclusion chromatography with inline multiangle light scattering and isothermal titration calorimetry to demonstrate that one PG9 binds per trimer by making contact between one PG9-Fab region and two of the three protomers of an artificially stabilized gp140 trimer. In analogy to the analyses employed to define the mode of V3 shielding by V1V2, experiments relying on mixed trimers can be employed to test whether quaternary epitopes are formed by intra-protomer (*non-shared epitopes, no cross-linking*) or inter-protomer (*shared, cross-linking*) interactions within the intact trimer (see Figure 1B).

The experimental basis of mixed trimer formation appear to be simple. The co-transfection of two envelope protein encoding plasmids at specific ratios seem to lead to the formation of mixed trimers reflecting these ratios. However, a multitude of random processes can occur during mixed trimer formation which can lead to differential expression profiles [43, 45]. A verification that trimer formation occurs at the desired molecular ratios is complex and requires both experimental analysis and employment of mathematical models to interpret data obtained from any such experimental system.

In the following, we describe and compare the two main approaches that have been used to answer specific questions about HIV envelope trimer function during entry and its inhibition by antibodies. In the recent literature, two experimental system have been employed for these types of questions. Here, we review these approaches and the corresponding models to reveal the advantages and disadvantages of either framework.

In particular, we address three major issues about these approaches: (i) Searching for the optimal experimental setup: Which experimental approach based on mixed trimer analysis is suited best to address molecular interactions of trimer protomers and antibodies? (ii) Deviation from the "ideally mixed" trimer: Several factors potentially influence the assembly of mixed trimers [43, 45]. We outline in detail how our model framework can be employed to test the effect of different assumptions concerning trimer formation on the predictions of experimental outcomes. (iii) We further demonstrate how our framework can be extended to study the contribution of individual envelope glycoproteins to the formation of quaternary epitopes (see Figure 1 B). These approaches make it possible to verify and define quaternary HIV Env specific antibodies and in particular to define whether epitopes of these antibodies are shared between neighboring protomers or originate from one protomer within the trimer.

2. Materials and Methods

In this section we describe the general experimental setup to study envelope trimer functions in the context of antibody binding and neutralization. In our approach each trimer species is displayed in a trimer table and rated

for functionality. Type, frequency and functionality of the trimer species are then translated into mathematical equations to predict the outcome of a certain experimental setup. These predictions indicate which experimental setups can be used to gain insights into specific aspects of inter- and intra-protomeric envelope functions.

2.1. Experiments

In principle two types of experimental approaches can be used to study inter- and intra-trimeric functions in the context of antibody binding and neutralization. In the first approach, antibody binding to mixed trimers expressed on transfected cells can be analyzed by flow cytometry. We refer to this approach in the following simply as *binding assays* (see also Figure 2 A). In the second approach, infectivity of pseudotyped virions expressing mixed trimers is evaluated in presence and absence of neutralizing antibodies. We refer to this experimental approach in the remainder of our study as *infectivity assays* (see also Figure 2 B).

In both experimental approaches mixed trimers are generated by co-transfecting suitable human cell lines with two different plasmids each encoding for another envelope variant [12, 67, 86–88]. For a typical experiment, a range of separate transfection reactions will be performed in parallel with varying the ratios of one envelope variant to the other. A central assumption of these experiments is that both plasmids enter the cells equally efficiently and are transcribed and translated at the same rate, such that the production of both envelope variants within the cells is reflected by the ratio of the transfected plasmids. Further, it is assumed that both envelope variants trimerize perfectly randomly, such that the proportions of the different homo-

and heterotrimers displayed on the transfected cell or the pseudotyped virion can again be predicted by the ratio of transfected envelope plasmids.

For binding assays, cells are transfected with the envelope plasmids only, which results in expression of envelope trimers on the cell surface. Domains or epitopes of interest on these mixed trimers can then be analyzed by flow cytometry utilizing fluorescently labeled Env specific antibodies (see Figure 2 A). It is assumed that the measured fluorescence intensity of a cell population is directly correlated with the availability of epitopes on the trimers that the respective antibodies are directed to. The mean fluorescence intensity, MFI, of a cell population expressing mixed trimers is obtained by subtracting the mean of the background signal (obtained from mock-transfected cells) from the mean of the cellular signal of the population expressing mixed trimers (for a schematic see Figure 3). Of note, Env proteins on transfected cells and virions are known to build intact trimers but also partially shed spikes, containing only one or two gp120 proteins. As in these incomplete spikes antibodies might also have access to epitopes that are not accessible in the intact trimers, the MFI must be corrected for this additional binding.

For the infectivity assays, pseudotyped virus is produced by additionally co-transfecting an env-deleted HIV proviral plasmid which results in the production of single-round infection competent, envelope pseudotyped virus (pseudovirus). For infectivity assays, the generated pseudotype virus stocks expressing different ratios of mixed trimers are subjected to saturating antibody concentrations and their capability to infect a target cell line is determined. In essence any susceptible target cell can be used in these studies and HIV infection monitored by various means e.g. HIV antigen production,

viral RNA quantification, or reporter gene expression. A convenient and often used target cell line for HIV neutralization assays are TZM-bL cells, which express firefly luciferase upon HIV infection and thus allow rapid and quantitative monitoring of HIV infectivity [50, 78]. Figure 2 outlines the basic features of the two setups. Binding assays were performed in [62] whereas infectivity assays were performed in [40] to study the mode of protection the V1V2-loop confers.

2.2. Analysis of trimer functionality using trimer tables

To study inter- and intra-protomeric functions in the context of antibody binding and neutralization, mixed trimers are used in experimental setups as described above. The two envelope proteins used must vary in their specific characteristics, such as presence or absence of a given epitope or of variable loops. Let us first consider an analysis of the mode of interaction between the V1V2 and V3 loops, i.e. dissection of neighboring (trans) or self (cis) interaction. To address this question, the envelope subunits in the mixed trimers must have different features: the V1V2 loop must either be present or deleted and the antibody binding site must either be antibody binding sensitive or defective. In more theoretical terms this means that there is a locus a in the envelope protein with two different variants a_1 and a_2 and another locus b with two variants b_1 and b_2. For example, locus a_1 can be engineered to delete the envelope V1V2 while locus a_2 carries the intact V1V2 domain. In analogy, the envelope variant b_1 encodes for a mutation in V3 rendering this protomer resistant to antibody binding while b_2 encodes for the antibody sensitive wild-type. Since there are two loci with two different variants each, there are $2^2 = 4$ possible envelope protein combinations. For

generating mixed trimers, two envelope proteins out of the four possible combinations are chosen for an experimental setup. Thus there are theoretically $\binom{4}{2} = 6$ possible experimental setups.

However, not all theoretically possible experimental setups contain the information necessary to distinguish between own or neighboring interaction. An easy tool to decide whether an experimental setup contains enough information to distinguish the different scenarios is a trimer table as presented in Figure 4. A trimer table lists all the different mixed trimers that can be formed in one specific experimental setup and also includes the antibodies bound depending on the different hypotheses to test. If there is at least one trimer which differs in its functions depending on the hypotheses that shall be tested, the setup can be used to test these hypotheses. There are only two out of the six theoretical envelope combinations fulfilling this condition for our example of the V1V2-V3 interaction.

Figure 4 contrasts trimer tables for binding assays with those for infectivity assays in three theoretically possible setups. Setup I and II can be used to infer the mode of interaction between V1V2 and V3, whereas setup III cannot be used for this purpose. This is because the different trimers in setup III have the same functionality for the two different interaction hypotheses, i.e. the trimer tables are identical for both hypothesis. Which of the two assays, binding or infectivity, is more suitable is discussed below.

Trimer tables can also help in other experimental setups. To dissect whether quaternary epitopes are constituted of components belonging to neighboring envelope proteins within the trimer, an experimental setup including envelope variants with defects in the epitopes must be used. An

example of a trimer table reflecting this situation can be found in Figure 9 B.

2.3. Models

The trimer tables must be transformed into mathematical formula to predict the behavior of different trimer combinations under different hypothetical assumptions. As the exact number of trimers expressed on a single transfected cell or on an individual pseudotyped virion is not known and cannot be precisely determined, the conducted experiments will only inform about trimer functionality and virion infectivity averaged over all trimers and virions of a population, respectively. Therefore, it is necessary to perform experiments with different envelope variant ratios and assess the qualitative change of the average number of antibodies bound in binding assays or the relative infectivity in infectivity assays, respectively.

In this section we describe the general assumptions of the models. We then derive the probability to form a trimer with a specified envelope composition. This probability forms the basis of models for binding and infectivity assays. In the section "Infectivity assays" we derive the relative infectivity measured in infectivity assays. The relative infectivity measures how well a virus stock expressing mixed trimers infects target cells under saturation of antibodies in comparison to the stock in absence of antibodies. In the section "Binding assays" we derive the normalized mean fluorescence intensities measured in binding assays. This measure informs about the average number of antibodies bound to cells expressing mixed trimers. In the sections "Considering imperfect transfection" and "Considering envelope segregation" we derive models under relaxed assumptions concerning trimer formation.

The models presented here are built on the following assumptions:

1. A sufficiently high number of envelope encoding plasmids enters the transfectable cell. This guarantees that the plasmids inside the cell have the same relative composition as outside, adjusted at the beginning of the transfection. This assumption is relaxed in the imperfect transfection model.
2. Plasmids are translated into proteins and trimers are formed from the envelope protein pool within the cell.
3. Three envelope proteins are chosen perfectly randomly to build a trimer out of the envelope pool. This assumption is relaxed in the segregation model.

In a system with two different envelope proteins A and B, we denote the fraction of envelope encoding plasmid with f_A and $f_B = 1 - f_A$, respectively. Under the above assumption the number of envelope proteins of type A follows a binomial distribution with parameters 3 and f_A, i.e. the probability that $k = 0, 1, 2, 3$ envelope proteins within one trimer are of type A is

$$\binom{3}{k} f_A^k (1 - f_A)^{3-k} \tag{1}$$

All parameters used are listed in table 1.

2.3.1. Infectivity assays

For infectivity assays we can predict the relative infectivity of pseudotyped virus stocks in the presence of monoclonal antibodies. Following the concept of stoichiometries, a virion is only able to infect a cell when at least T functional trimers attach to cell receptors. A trimer is functional when less than N antibodies are bound to the trimer [28, 29, 43, 45, 67, 86, 87]. Virions vary in trimer expression and the fraction of virions that express s

trimers is η_s for $s = 0, 1, \ldots, s_{\max}$. For all predictions of the relative infectivity in infectivity assays we use $s_{max} = 100$ and a discretized beta-distribution with mean 14 and variance 49. This distribution is based on trimer number counts on HIV-1 virions [91], and details of its definition are laid out in [45]. Let f_A be the fraction of envelope encoding plasmids with binding sensitive epitopes. The relative infectivity for a binding scenario S can then be derived according to [43, 45]

$$\mathrm{RI}(S, T, N, \eta, f_A) = \frac{\sum_{s=T}^{s_{\max}} \eta_s \left(\sum_{g=T}^{s} \binom{s}{g} {\alpha_{S,N}}^g (1 - \alpha_{S,N})^{(s-g)} \right)}{\sum_{k=T}^{s_{\max}} \eta_k} \qquad (2)$$

where $\alpha_{S,N}$ is the probability that a functional trimer forms given the stoichiometry of neutralization N and the scenario S. This can be calculated by summing over the probabilities to form a functional trimer with k type A envelope proteins (equation 1). As an example of how $\alpha_{S,N}$ can be calculated we look at infectivity assays in setup I (first row, second column in figure 4). All trimers are functional (indicated by "+") except the heterotrimers in the neighboring scenario assuming that one antibody is enough to neutralize a trimer (i.e. $N = 1$). The probability that a functional trimer forms under these assumptions is the sum of forming homotrimers. Applying equation 1, we obtain

$$\alpha_{\mathrm{neigh},1} = \binom{3}{0} f_A^0 (1 - f_A)^{3-0} + \binom{3}{3} f_A^3 (1 - f_A)^{3-3} = (1 - f_A)^3 + f_A^3$$

where type A envelope proteins are antibody binding sensitive and have the V1V2 loop.

2.3.2. Binding assays

For binding assays we predict the normalized mean fluorescence intensity for a series of cell populations expressing mixed trimers. Each cell population is produced with a certain fraction of type A encoding plasmids. We obtain a curve of the normalized mean fluorescence intensity as a function of the fraction of type A envelope proteins. To derive this curve, we first define X as the number of antibodies binding to one random trimer. The mean number of antibodies binding to one trimer given the fraction of type A envelope proteins, f_A, is then:

$$EX = \sum_{k=0}^{3} n_k P(X = k) = \sum_{k=0}^{3} n_k \binom{3}{k} f_A^k (1 - f_A)^{3-k} \tag{3}$$

where n_k denotes the number of antibodies that bind to a trimer with k type A envelope proteins, for $k = 0, \ldots, 3$. The *normalized mean fluorescence intensity*, nMFI, is a function in f_A and $\mathbf{n} := (n_0, n_1, n_2, n_3)$:

$$\mathrm{nMFI}(\mathbf{n}, f_A) = \frac{1}{\max\limits_{x \in [0,1]} \{\sum_{k=0}^{3} n_k \binom{3}{k} x^k (1-x)^{3-k}\}} \sum_{k=0}^{3} n_k \binom{3}{k} f_A^k (1 - f_A)^{3-k} \tag{4}$$

where $\mathbf{n}$ must be determined via the trimer tables and thus depends on the particular hypothetical scenario. For example, in binding assays and setup I (first row, first column in figure 4) $\mathbf{n} = (0, 1, 1, 0)$ in the neighboring protection scenario and $\mathbf{n} = (0, 0, 0, 0)$ in the self protection scenario.

2.3.3. Considering imperfect transfection

In the models described above we assumed that the fraction of type A envelope proteins in the envelope pool is equal to the fraction of type A encoding plasmids that were transfected. If only a few plasmids can enter

the cell or the expression of one plasmid is favored over the other, the fraction of type A envelope proteins in the envelope pool differs from f_A. We extend the basic model to allow imperfect transfection, or more general variation between the envelope pool and the plasmid ratios [43, 45]. We described models considering imperfect transfection in the context of the stoichiometry of entry and neutralization [43, 45] and in the context of V1V2 loop protection [62] earlier. Here we show how the mean fluorescence intensity and the normalized mean fluorescence intensity can be derived in these model extensions and which additional information can be obtained by studying the (non-normalized) mean fluorescence intensity.

We model the fraction of type A envelope proteins in the envelope pool as a B-distributed random variable F_A with mean $f_A \in (0,1)$ and variance

$$v = \tilde{v} f_A (1 - f_A) \tag{5}$$

where $\tilde{v} \in (0,1)$ denotes the *coefficient of variation*.

In the models for infectivity assays, the probability that a functional trimer forms, $\alpha_{S,N}$, in equation 2 has to be adapted. Trimerization is again assumed to be binomial but now with the distribution $\mathcal{B}(3, F_A)$. Thus, the probability that an average trimer has $k = 0, 1, 2, 3$ type A envelope proteins is

$$\int_0^1 \binom{3}{k} x^k (1-x)^{3-k} \beta_{f_A,\tilde{v}}(x) \mathrm{d}x \tag{6}$$

$\beta_{f_A,\tilde{v}}$ is the probability density function of a B-distribution with mean f_A and coefficient of variation $\tilde{v}$ which is equivalent to a B-distribution with

parameters p and q, given the definitions

$$\begin{aligned} p &:= \frac{f_A^2 - f_A^3 - \tilde{v} f_A^2 (1 - f_A)}{\tilde{v} f_A (1 - f_A)} \\ q &:= \frac{f_A - 2f_A^2 + f_A^3 - \tilde{v} f_A (1 - f_A) + \tilde{v} f_A^2 (1 - f_A)}{\tilde{v} f_A (1 - f_A)} \end{aligned} \tag{7}$$

This equivalence holds because the B-distribution with parameters p and q has mean $\frac{p}{p+q}$ and variance $\frac{pq}{(p+q+1)(p+q)^2}$. Hence

$$\mathrm{RI}_{itm}(S, T, N, \eta, f_A, \tilde{v}) = \frac{\sum_{s=T}^{s_{\max}} \eta_s \left(\sum_{g=T}^{s} \binom{s}{g} \alpha_{S,N}^{itm\, g} (1 - \alpha_{S,N}^{itm})^{(s-g)} \right)}{\sum_{k=T}^{s_{\max}} \eta_k} \tag{8}$$

where $\alpha_{S,N}^{itm}$ is the probability that a trimer is functional given the scenario S and the stoichiometry of neutralization N.

In binding assays, we replace the fraction of type A envelope proteins, f_A, in equation 4 by the random variable F_A. By taking the mean, we obtain for the normalized mean fluorescence intensity in the imperfect transfection model:

$$\mathrm{nMFI}^{\mathrm{itm}}(\mathbf{n}, f_A) = \frac{1}{\max\limits_{x \in [0,1]} g^{\mathrm{itm}}(\mathbf{n}, x, \tilde{v})} g^{\mathrm{itm}}(\mathbf{n}, x, \tilde{v}) \tag{9}$$

with

$$g^{\mathrm{itm}}(\mathbf{n}, x, \tilde{v}) = E\left(\sum_{k=0}^{3} n_k \binom{3}{k} F_A^k (1 - F_A)^{3-k} \right) \tag{10}$$

Because $EX^n = (EX)^n$ only if $VarX = 0$, imperfect transfection will have an influence on the predictions for the normalized mean fluorescence intensity. However, this influence decreases when the coefficient of variation goes to 1 (which also implies that the variance of F_A goes to 1).

In addition to the normalized mean fluorescence intensity, the (non-normalized) mean fluorescence intensity adds to the understanding of po-

tential imperfect transmission. The (non-normalized) mean fluorescence intensity is the same as $g^{\mathrm{itm}}(\mathbf{n}, x, \tilde{v})$ shown in equation 10. For a coefficient of variation close to 1, almost every cell is transfected with only one type of envelope encoding plasmid. Hence, most of the cells express only one type of homotrimers. The few cells that are transfected with two types of envelope encoding plasmids have a huge variation in the composition of heterotrimers. If imperfect transfection plays a role in the generation of mixed trimers, this effect must be reflected in flow cytometry readouts.

2.3.4. Considering envelope segregation

During the formation of mixed trimers, it could be possible that homotrimers are preferentially built. In this case, trimer formation would not happen perfectly randomly, i.e. may not follow a binomial distribution [43, 45]. In the following, we extend the models for the relative infectivity and the mean fluorescence intensity to incorporate this possibility. To this end, we introduce a parameter $\xi \in [0, 1]$ describing the degree of segregation of two envelope variants towards homotrimers. $\xi = 0$ means that there is no segregation and trimer formation occurs according to a binomial distribution. $\xi = 1$ describes a scenario in which only homotrimers are formed. In the extended model, trimer formation is conceived as the successive addition of envelope proteins. The incorporation of an envelope protein of the same type as the previous one is more likely than the incorporation of one of a different type. If we denote the fraction of type A envelope proteins in the envelope pool as f_A, the probability of incorporating another envelope of type A is $f_A^{1-\xi}$. Thus, the probability that a trimer has three type A envelope

proteins is

$$P_3 = f_A f_A^{1-\xi} f_A^{1-\xi} = f_A^{3-2\xi} \tag{11}$$

Similarly, the probability that an envelope protein of type B is incorporated when there is already one of this type in the trimer is defined as $(1-f_A)^{1-\xi}$. Thus, the probability that a trimer has three type B proteins, or no type A protein, is

$$P_0 = (1-f_A)^{3-2\xi} \tag{12}$$

The probabilities P_k that a trimer forms with $k = 1, 2$ type A envelope proteins can similarly be derived as:

$$\begin{aligned} P_1 &= f_A \left(1 - f_A^{1-\xi}\right)^2 + 2(1-f_A)^{2-\xi}\left(1-(1-f_A)^{1-\xi}\right) \\ P_2 &= (1-f_A)\left(1-(1-f_A)^{1-\xi}\right)^2 + 2f_A^{2-\xi}\left(1-f_A^{1-\xi}\right) \end{aligned} \tag{13}$$

Equations 11 – 13 define a valid probability distribution, because $0 \leq P_k \leq 1$ for $k = 0, 1, 2, 3$ and the probabilities sum to 1 (see also [43]).

Replacing the probabilities to form a trimer with k type A envelope proteins in equation 2 leads to the following prediction of the relative infectivity in infectivity assays

$$\mathrm{RI}_{seg}(S, T, N, \eta, f_A) = \frac{\sum_{s=T}^{s_{\max}} \eta_s \left(\sum_{g=T}^{s} \binom{s}{g} \alpha_{S,N}^{seg\ g} (1-\alpha_{S,N}^{seg})^{(s-g)}\right)}{\sum_{k=T}^{s_{\max}} \eta_k} \tag{14}$$

where $\alpha_{S,N}^{seg}$ is the probability that a trimer is functional given the scenario S and the stoichiometry of neutralization N. This probability can be obtained by summing over all probabilities P_k of trimers with k type A envelope proteins that are functional.

If we apply this to infectivity assays in setup I (first row, second column in figure 4) $\alpha_{\mathrm{neigh},1}^{seg} = P_1^3 + P_2^3$ and equals one for the stoichiometries of

neutralization $N = 2$ and $N = 3$ in the neighboring protection scenario as well as for all stoichiometries of neutralization in the self protection scenario. Type A envelope proteins are V1V2 deleted and antibody binding resistant in this example.

The mean fluorescence intensity in binding assays for the imperfect transfection model is similarly derived by replacing the probability that a trimer with k type A antibodies forms in equation 4 with the probability P_k derived in equations 11 – 13. Thus

$$\mathrm{nMFI}_{seg}(\mathbf{n}, f_A) = \frac{1}{\max\{\sum_{k=0}^{3} n_k P_k\}} \sum_{k=0}^{3} n_k P_k \tag{15}$$

The vector $\mathbf{n}$ containing the numbers of antibodies that bind to a trimer with k type A envelope proteins must be read out of a trimer table.

With increasing segregation, i.e. $\xi \to 1$, fewer heterotrimers will be expressed on the cell surface. If the number of antibodies binding to homotrimers differs from the number of antibodies binding to hetereotrimers, the intensity of the fluorescence signal will change across different cell lines expressing different mixtures of envelope proteins. Therefore one can also gain insight into the process of segregation by looking at the (non-normalized) mean fluorescence intensity:

$$\mathrm{MFI}_{seg}(\mathbf{n}, f_A) = \sum_{k=0}^{3} n_k P_k \tag{16}$$

3. Results

3.1. Analysis of protomer interactions within trimers using binding and infectivity assays

In Figure 5 we show the theoretical predictions for six different experimental systems. Each row corresponds to a different combination of two envelope proteins. The mixed trimers expressed on envelope plasmid transfected cells are subjected to an antibody which targets an epitope of interest at saturating concentrations and cells are analyzed for antibody binding by flow cytometry. The predictions for the normalized mean fluorescence intensity, nMFI, as a function of the fraction of type A envelope proteins for the different binding scenarios is shown in the column "binding assay". If the envelope plasmid transfected cells are additionally transfected with plasmids encoding for the viral genome, pseudotyped virions expressing mixed trimers are produced. These pseudotype virus stocks are subjected to saturating antibody concentrations and their capacity to infect target cells is assayed. The predictions for the relative infectivity, i.e. the infectivity of a pseudotyped virus stock reacting with antibodies divided by the infectivity of the same virus stock without antibodies, are shown in the column "infectivity assays". For these predictions we assumed a stoichiometry of entry $T = 8$, an estimate we obtained in [45] for the basic model. The predictions shown in figure 5 correspond to the trimer tables in figure 4.

3.1.1. Binding assays

Predictions for this assay type are shown in the column "binding assays" in figure 5 and this paragraph refers to binding assays only. Setup III can be

used as a control setup, because the different interaction scenarios between V1V2 and V3 are not distinguishable. In setup I and II, the different interaction scenarios are predicted to result in clearly distinguishable normalized mean fluorescence intensity curves. If the interaction between V1V2 and V3 is inter-protomeric (neighboring/ trans protection), we expect a hump-shaped curve for the normalized mean fluorescence intensity as a function of the fraction of V1V2 deleted, antibody resistant envelope proteins in setup I, compared to a flat line (i.e. no antibody binding to any trimer) for own protection. In setup II, we expect a bow-shaped curve for neighboring protection, compared to a linear relationship between antibody binding and the fraction of V1V2 deleted - antibody sensitive envelope proteins for own protection. We previously confirmed these predictions experimentally [62].

3.1.2. Infectivity assays

Predictions for this assay type are shown in the column "infectivity assays" in figure 5. This paragraph refers to infectivity assays only. As mentioned above, we assume $T = 8$ for the predictions in figure 5 in accordance with the estimates for the basic model, i.e. the model assuming perfectly random trimer formation and no segregation nor imperfect transfection [45]. The predictions for the different relative infectivities not only depend on the hypothesized mode of interaction between V1V2 and V3, but also on stoichiometric parameters. In setup I, we predict constant relative infectivity of 100% for self (cis) protection for all stoichiometries of trimer neutralization $N = 1, 2, 3$ but we also predict the same straight line for neighboring (trans) protection for $N = 2$ and $N = 3$. Only in case $N = 1$, our model predicts a valley-shaped curve for neighboring protection. This means that the mode of

V1V2 interaction with V3 can only be inferred with setup I if the monoclonal antibody used in the experiments has a $(N = 1)$-stoichiometry. Infectivity assays as shown in setup II also yield ambiguous results. Only if the data fits the self protection and $(N = 1)$-curve, can one deduce self protection and $N = 1$. If the stoichiometry of neutralization is known and is either $N = 1$ or $N = 2$, the mode of protection can be distinguished according to the relative infectivity curves. In addition, the stoichiometry of entry, T, has a strong influence on the model predictions in both setups. In setup I the valley is the deeper, the higher the entry stoichiometry, T is as we show in figure 6 (A). In setup II we can see that the higher T is, the more are all relative infectivity curves shifted to the left (shown in Figure 6 (B)). Therefore it is possible that relative infectivity curves for different parameter sets and mode of protections are identical making it impossible to determine the mode of V1V2 protection without prior knowledge of stoichiometric parameters.

In addition to uncertainties related to the stoichiometries of entry and neutralization, the distribution of the number of trimers across different virions has a huge impact on the predictions of the relative infectivity curves, as shown in [28, 43, 45]. The more trimers a virion displays on average, the more are the relative infectivity curves shifted to the right. The variation in the trimer number distribution influences the slope of the relative infectivity curves. Neither the stoichiometries of entry and neutralization nor the distribution of trimer numbers are conclusively determined yet. Therefore, different modes of V1V2 interaction with V3 cannot clearly be distinguished in infectivity assays. Binding assays, on the other hand, do not include the infection step and therefore all ambiguities associated with this step such

as the trimer number distribution on virions as well as the stoichiometry of entry and neutralization, do not affect the predicted normalized mean fluorescence intensity curves. Therefore, we only consider binding assays in the following sections.

3.2. Testing different assumptions concerning trimer formation

In Figure 7 we show how imperfect transfection and segregation influence the predictions for the normalized mean fluorescence intensity for experimental setup I (in figure 4). If the transfection of cells with envelope encoding plasmids is imperfect, the predictions for the normalized mean fluorescence intensity for both modes of V1V2 interaction with V3 are the same as for the basic model tested above (figure 7 A). However, if the self protection scenario holds true, higher segregation coefficients broaden the normalized mean fluorescence curves for the neighboring protection scenario. The predictions for the self protection scenario is not affected by segregation (figure 7 B).

The normalized mean fluorescence intensity neglects variation in the strength of fluorescence signals that might include additional information. The fluorescence signal in binding assays for neighboring protection in setup I comes from antibodies binding to heterotrimers with one or two V1V2 expressing and antibody binding sensitive envelope proteins (see Figure 4). Both model extensions accounting for imperfect transfection and segregation for the *normalized* mean fluorescence intensity (equations 9 and 15) predict a hump shaped curve for any coefficient of variation, $\tilde{v}$, and segregation parameter, ξ. However, the expression of heterotrimers expressed decreases with increasing $\tilde{v}$ as well as increasing ξ. This leads to a reduction of the mean fluorescence intensity measured with flow cytometry. We predict this effect

in figure 8 for the model extensions accounting for imperfect transfection (A) and segregation (B). The decrease in MFI signal can be used to study potential imperfect transfection or segregation. Here, we demonstrate how segregation can be addressed experimentally, imperfect transfection can be studied similarly.

3.2.1. Test for segregation in setup I

As demonstrated in [62] binding assays in setup I (mixing V1V2 deleted, antibody binding resistant envelope proteins with V1V2 expressing, antibody sensitive envelope proteins) lead to a hump-shaped curve for the normalized mean fluorescence intensity. This result is only in accordance with our model predictions for the neighboring protection scenario in which only heterotrimers can be bound by one antibody. According to equation 16, the mean number of antibodies per trimer is:

$$1 - f_A^{3-2\xi} - (1 - f_A)^{3-2\xi} \tag{17}$$

When mixing the two different envelope proteins in equal amounts, f_A equals 0.5 and equation 17 simplifies to $1 - 0.5^{2-2\xi}$. If there was segregation, we predict lower mean fluorescence intensity of a cell population expressing a 1:1 mix of the two different envelope proteins in comparison to the mean fluorescence intensity of a 100% antibody binding sensitive trimer expressing cell line. The higher the segregation parameter is, the lower is the mean fluorescence intensity of a mixed trimer expressing cell population (down the grey line in figure 8). Therefore, the factor with which the mean fluorescence intensity of a 100% antibody binding sensitive cell population is higher than the mean fluorescence intensity of a mixed envelope trimer expressing pop-

ulation increases with increasing segregation parameter ξ. This consequence of the mathematical model is shown in Figure 8 C. We experimentally determined the mean fluorescence intensity of four independent cell populations with a 1:1 ratio of V1V2-deleted, antibody binding resistant envelope proteins mixed with V1V2-present, antibody binding sensitive envelope proteins. Simultaneously with the mixed trimers expressing cell populations, we tested a cell population expressing 100% antibody binding sensitive expressing cell populations as controls. We find that the mean fluorescence intensity of the control populations is on average 2.7 times higher than the mixed trimer expressing cell populations (variance of 0.729). This is not as high as the predicted factor, which is 4 times higher, but clearly smaller than this factor. Only a higher factor is a proof of segregation (see Figure 8 C). This strongly suggests that there is no bias towards homotrimers in the mixed trimer system employed here. On the basis of a similar calculation this data also suggests that there is no imperfect transfection.

When comparing the effects of imperfect transfection and segregation on the predictions for the normalized and the non-normalized mean fluorescence intensity, it seems as if both scenarios have the same effect. However, the two scenarios are different in terms of the expression level of mixed trimers on the cellular surface. In case of complete imperfect transfection ($\tilde{v} = 1$), each cell is transfected with only one type of plasmid and therefore expresses only homotrimers of one sort. In the experimental setup I, homotrimers cannot be detected by flow cytometry. When the coefficient of variation is slightly smaller than one, there are only very few cells transfected with both types of plasmids. These cells then express heterotrimers which can be detected by

flow cytometry. Hence, in case of imperfect transfection, most of the cells are not detected by flow cytometry, because they do not express heterotrimers. In contrast, in the segregation model all cells are transfected with a mixture of envelope encoding plasmids that represents the experimentally adjusted ratios. With increasing segregation parameter, the formation of homotrimers becomes more likely. However, a small percentage of the expressed trimers are heterotrimers. This leads to a weaker fluorescence signal per cell but most of the cells express hetereotrimers. In summary, if the mean fluorescence intensity of cells expressing mixed trimers is much smaller than the calculated reduction compared to a 100% sensitive envelope trimer expressing cell, imperfect transfection or segregation could be the explanation. If most of the cells cannot be detected in flow cytometry, imperfect transfection is the most likeliest explanation for the overall reduction of the mean fluorescence intensity. If, however, most of the cells show a fluorescence signal, segregation is the most likeliest explanation.

3.3. Defining inter- and intraprotomeric quaternary epitopes of envelope specific antibodies

Neutralizing antibodies which bind to quaternary epitopes have been identified in recent years and are of considerable interest due to their potent and broad activity [19, 60, 76]. In theory, the quaternary epitopes of these antibodies can be constituted by components of the same envelope protein protomer (non-shared epitope, no cross-linking) or components from neighboring protomers within the trimer (shared epitopes, cross linking); figure 1B illustrates these two concepts. Walker et al. [76] studied the binding of PG9 and PG16 to mixed trimers expressed on cells using a similar

approach as presented here. However, in that study, only a 1:2 ratio of wild-type to mutant, antibody binding resistant envelope protein was used to test for quaternary epitopes. The mean fluorescence intensity of a cell population expressing mixed trimers with the 1:2 envelope ratio was compared to the mean fluorescence intensity of a 100% wild-type expressing cell population. With this approach, Walker et al. concluded that PG9 and PG16 bind to a quaternary structure of the envelope trimer that is not constituted by direct inter-protomeric envelope interactions (i.e. non-shared epitopes, no cross-linking). In contrast, [27] concluded from electron microscopic reconstructions that a single Fab region of PG9 binds asymmetrically to two envelope subunits.

In this section we describe how the binding assay approach for studying the mode of V1V2 interaction with V3 can be extended to study inter- and intraprotomeric interactions for quaternary epitopes. This approach has the advantage that it not only relies on one ratio of wild type and mutant encoding plasmids, but also on several cell populations expressing different ratios. Figure 9 illustrates this concept. Figure 9 A shows a 2-dimensional sketch of an antibody binding to an epitope that is only part of one envelope protein (non-shared epitope) and of an antibody binding to an epitope consisting of two parts that are distributed over two neighboring envelope proteins (shared epitopes).

To study shared/non-shared epitopes, binding assays with cells expressing mixed envelope trimers in combination with our model framework can be used. The two envelope proteins being employed in these experiments are (i) wild-type envelope protein to which the antibody can bind (ii) an envelope

mutant with mutations in the epitope regions making the protein antibody binding resistant (Figure 9 A). As described above, four different types of mixed trimers will be generated when plasmids encoding for the two different envelope proteins are co-expressed in a transfected cell. For the binding assay, fluorescently labeled antibodies bind to the functional epitopes. If the epitope is part of only one envelope protomer, the number of antibodies that can bind to one trimer is equal to the number of wild-type envelope proteins in this trimer. On the other hand, under the assumption that there is no steric hindrance, three antibodies bind to trimers with three wild-type envelope proteins, one antibody binds to trimers with two wild-type envelope proteins and 0 antibodies to the other trimers if the epitope is shared between two envelope proteins (Figure 9 B).

In equation 4, we derived the normalized mean fluorescence intensity for perfectly random trimer assembly which can be used to predict the normalized mean fluorescence intensity for the shared and non-shared epitope hypothesis. According to the trimer table in figure 9, the number of antibodies binding to the different trimers for the non-shared scenario and the shared scenario are $\mathbf{n}_1 = (3, 2, 1, 0)$ and $\mathbf{n}_2 = (3, 1, 0, 0)$, respectively. f_A is the fraction of antibody binding resistant envelope proteins. The predicted normalized mean fluorescence intensity, nMFI, for both scenarios are shown in Figure 9 (C). If the epitope is located on only one envelope protein, we predict a straight line for the nMFI as a function of the fraction of mutant envelope proteins. In the case that the epitope is formed from components belonging to two envelope protomers, we predict a bow-shaped curve. The two curves are clearly distinguishable. It is therefore possible to determine

whether an epitope is located on only one envelope protein or shared between two envelope proteins within the trimer.

3.3.1. Advantages and disadvantages of binding and infectivity assays

In this section we discuss the advantages and disadvantages of binding and infectivity assays (additionally summarized in table 2).

Binding assays. In general, binding assays are useful when studying the number of antibodies bound to trimers. The assays average over a high number of trimers, and can be applied to determine the modes of shielding epitopes from antibody binding or the composition of quaternary epitopes. As, in this assay, trimer functionality is measured when trimers are expressed on the cell surface, questions related to the role of trimers in the infection process cannot be addressed. Therefore, stoichiometric questions related to the infection process cannot be studied by binding assays. The analysis of binding assays can be confounded by segregation and imperfect transfection but these effects can be accounted for with the mathematical model described above. Different trimer expression levels are only reflected in the non-normalized mean fluorescence intensity but not in the nMFI. If partially shed trimers are expressed on the cell surface, which are known to be more accessible to antibody binding, the models for binding experiments must be adapted as shown in [62]. If antibodies can additionally bind unspecifically, the background signal will be higher but will not influence the overall patterns for the nMFI of differently mixed trimers.

Infectivity assays. In general, infectivity assays are of great importance when the function of trimers in the infection process is studied, e.g. in determining

stoichiometries. However, when using these assays to infer the mode of protection from antibody binding conferred by the V1V2 loop, or the location of quaternary epitopes in infectivity studies additional knowledge is required. In particular, information about the number of trimers is needed for cell entry (stoichiometry of entry) and the number of antibodies required to neutralize a single trimer (stoichiometry of trimer neutralization) is essential.

As for binding assays, potential segregation and imperfect transfection constitute confounding factors, for which the mathematical analysis can correct. In contrary to binding assays, the positions of trimers on the virion might also play an important role in infection (see [43, 45]). In these studies we also extended the model for infectivity assays to account for a potential soft threshold of infection, in which the virion's ability to infect a target cell linearly increases with the number of trimers expressed on its surface. Because this soft threshold only plays a role in infection, we do not need to consider these potential confounding factors in binding assays.

Another important issue is that homotrimers of the two envelope variants used can have different expression levels, infectivities or stoichiometries of entry [6, 72, 73, 85]. This problem can be dealt with by either choosing envelope variants with similar features, or by adapting the models to account for this variation. Considering all these additional potential confounding factors, we suggest to use binding assays whenever determination of infectivity is not absolutely required.

4. Discussion

In this paper, we show how mathematical models can help to study the molecular interactions between the HIV envelope trimer and antibodies in the process of antibody binding and neutralization. As an example, we present a detailed model framework that allows the analysis of experimental data aimed at investigating the mode of interaction between the V1V2 and V3 loops within the HIV envelope trimer. In addition, this framework is extended to study the protomeric contributions to quaternary epitopes. We report here how such mathematical analyses of infectivity and binding assays can fill a methodological gap and reveal molecular aspects that evade direct observation by classical approaches such as crystallography or cryo-electron microscopy. In addition to providing a way to analyze experimental data after their generation, the mathematical models presented here allow us to identify the experimental approaches and the envelope mutants that are most promising to infer trimeric and protomeric functions for a more meaningful experimental design.

Mixed trimers either expressed on cells [62, 76] or on pseudotyped viruses [22, 40, 67, 86–88] form the basis of an experimental approach that can be applied to study various functions of the trimer in the entry process and its interaction with antibodies. Envelope-expressing cells can be saturated with fluorescently marked antibodies and antibody binding to the trimer can be tested with flow cytometry. If viruses are studied, they must be saturated with antibodies and then tested in infectivity assays. The most important twist of the infectivity and binding assays used for this purpose is the combination of different envelope proteins with different phenotypic characteristics,

for example absence/presence of the V1V2 loop or resistance/sensitivity to antibody binding.

For HIV, it has been shown that antibody binding to the spike is necessary and sufficient for neutralization [57, 65, 89]. Thus, antibody binding to the spike negatively correlates with the infectivity of a virus population. To understand how virions evade neutralization by antibodies might not require to study the whole infection process. In particular, the mode of protection by V1V2 and the formation of quaternary epitopes can be studied with the binding assay approach, because these processes only involve scoring of antibody binding and not the infection process. In binding assays it is possible to determine the number of antibodies bound to proteins expressed on the cell surface measuring the fluorescence intensity. This quantity is proportional to the number of intact binding sites. Since the number of trimers expressed on a single cell is unknown, the fluorescence signal cannot be directly translated into the number of antibodies bound to a single trimer. However, the change in the fluorescence intensity for different cell populations can be used for inference. This antibody binding based approach informs about the interaction between antibodies and the trimers. Dependent on the envelope variants used, different questions concerning the antibody/trimer interaction can be studied. Additionally the binding assay approach circumvents the uncertainties surrounding the infection process, namely quantitative information on the trimer number distribution, the stoichiometry of entry, T, and the stoichiometry of neutralization, N. However, with this approach it is not possible to study how the role of the trimer in the infection process changes upon antibody binding.

In contrast, approaches relying on infectivity assays have to face these uncertainties. The relative infectivity measured in such assays sensitively depends on the trimer number distribution and the stoichiometric parameters. Until now all efforts to estimate these parameters have been inconclusive [28, 43, 45, 67, 86, 87, 91], mostly because relative infectivity measures provide only limited, macroscopic information that is consistent with a multitude of assumptions about the molecular processes underlying neutralization and infection. On the other hand, infectivity assays recapitulate a larger part of the relevant viral life-cycle. Therefore, all questions related to the infectivity of viruses, e.g. the change of infectivity due to antibody binding, can be addressed with infectivity assays. We list the advantages and disadvantages of binding assays and infectivity assays and the questions that can be addressed with either approach in table 2.

While the binding assay approach circumvents uncertainties about parameters only needed in modeling the infection process, we still need to make assumptions about the molecular processes of envelope protein expression and trimer formation. In our model, we assume that enough plasmids enter transfectable cells to guarantee that the translated envelope proteins in the transfectable cells represent the mixture of plasmids at the beginning of the experiment. In the imperfect transfection model, we relax this assumption [43, 45]. Furthermore, we assume that trimers form randomly according to a binomial distribution from the envelope protein pool within transfected cells. In the segregation model we allow a bias towards homotrimer formation [43, 45]. These model extensions also predict hump-shaped curves for the normalized mean fluorescence intensity, nMFI, in binding assays with ΔV1V2,

antibody resistant envelope proteins and V1V2 expressing, antibody sensitive envelope proteins (setup I in figure 4). However, the fluorescence signal of the (non-normalized) mean fluorescence intensity for high segregation coefficients or coefficients of variance would be very small in comparison to the fluorescence signal of a 100% antibody binding sensitive cell population. According to our experimental data on the (non-normalized) mean fluorescence intensity we conclude that segregation as well as imperfect transfection are unlikely to occur in the system studied here.

Additional support for low segregation as well as imperfect transfection coefficients arise from studying the normalized mean fluorescence intensity for V1V2 deleted and antibody binding sensitive envelope proteins co-expressed with V1V2 present and antibody binding resistant envelope proteins (setup II in figure 4 and 5, [62]). In this setup, imperfect transfection would not change the predictions for the normalized mean fluorescence intensity. However, a high segregation coefficient would straighten the nMFI curve for the neighboring scenario. The data in [62] for this setup clearly shows a bow-shaped curve, and we therefore conclude that a high segregation coefficient, i.e. preferential formation of homo-trimers is unlikely. This conclusion is in apparent contradiction with our earlier findings in [45]. In that study, we re-analysed a data set by Yang et al. [87] to determine the stoichiometry of entry. When applying the segregation model, we estimated a high segregation coefficient. However, in the earlier study, a high segregation coefficient was only one of many ways to improve the fit of our models to the relative infectivity data. Other effects, such as proximity requirements of spikes for infection or soft thresholds, could also improve the model fit. Hence, we had

cautioned that the improvement of the model fits cannot be interpreted as evidence for any of these effects [45]. Besides theoretical caveats concerning the different estimates of the segregation coefficient, it might also be possible that different envelope variants used have different segregation behaviors.

In the recent literature several studies can be found which utilized the mixed trimer approach to investigate V1V2 loop interactions and quaternary epitopes. [40] studied V1V2 and V3 interactions with infectivity assays in a complementation system. The authors concluded that V1V2 interacts with the V3 loop of the same envelope protomer (self/cis protection). This study did not include mathematical modeling and did not consider that the stoichiometry of entry and neutralization can have a huge impact on the validity of the interpretation. [76] studied the number of subunits to which one monoclonal antibody - either PG9 or PG16 binds. The mean fluorescence intensity of one cell population expressing mixed trimers generated with a 1:1 ratio of wild-type and mutant envelope proteins was used to conclude that the quaternary epitopes of PG6 and PG19 are located on one protomer (non-shared epitope). This finding was supported by another approach where the neutralization potency of antibodies was tested for a number of pseudotyped virion populations expressing mixed trimers [13]. The latter study employed a best-fit approach without a conceptual mathematical model. However, [27] deduced that only a single PG9 binds to the whole trimer by asymmetrical interaction of one Fab region with two of the three protomers. In the present study, we derived another approach based on binding assays with mixed trimers to study the location of a quaternary epitope within the trimer. Overall, these approaches require a thorough mathematical analysis based on

models including a number of factors that can bias these type of analyses. Therefore we see a need for a more detailed assessment and verification of confounding factors in these type of studies.

A precise understanding of the architecture of the viral spike is urgently needed to rationally design vaccine immunogens that elicit potent neutralizing antibodies. While crystal structures of truncated envelope proteins and envelope proteins in complex with CD4 or antibodies as well as cryo-EM studies derived over recent years [24, 33, 39, 47, 79] have shed light on the molecular architecture of the HIV envelope proteins, much of the molecular details remain unknown. For instance, as outlined above, we still lack a detailed understanding of how precisely the protomers of gp120 interact within the trimer. In the intact trimer, some receptor binding sites are shielded both by glycan side chains and the variable loops V1V2. The latter potently protects the V3 loop within gp120. How precisely the V1V2 domain induces shielding has been elusive for a long time as both protection of the V3 loop by a neighboring V1V2 domain, or the V1V2 domain from the own protomer is conceivable. Identifying the position of V1V2 within the trimer remains of high interest as the V1V2 shielding is one of the most powerful protection mechanisms against neutralizing antibody attack the virus has evolved. Any successful neutralizing antibody regimen, be it prophylactic or therapeutic, will need to bypass this shield or as exemplified by the broadly neutralizing mAbs identified of late [76], utilize components of the V1V2 in binding to the trimer. Defining the precise position and structure of the V1V2 domain within the trimer is thus of outmost importance. We believe that a combination of experimental approaches and mathematical models as outlined

here, will shed light on these mechanisms. Our suggested framework is one step into this direction which we hope will be followed by further studies combining theory with experiments.

5. Acknowledgements

We gratefully acknowledge the Swiss National Science Foundation (SNF) and the Deutsche Forschungsgemeinschaft (DFG) for funding (CM: PBEZP3_137298 (SNF) and MA 5320/1-1 (DFG), AT: 310000-120739 (SNF), RRR: 315230-13085 (SNF)).

References

References

[1] Bar, K. J., Tsao, C. Y., Iyer, S. S., Decker, J. M., Yang, Y., Bonsignori, M., Chen, X., Hwang, K. K., Montefiori, D. C., Liao, H. X., Hraber, P., Fischer, W., Li, H., Wang, S., Sterrett, S., Keele, B. F., Ganusov, V. V., Perelson, A. S., Korber, B. T., Georgiev, I., McLellan, J. S., Pavlicek, J. W., Gao, F., Haynes, B. F., Hahn, B. H., Kwong, P. D., Shaw, G. M., 2012. Early low-titer neutralizing antibodies impede HIV-1 replication and select for virus escape. PLoS Pathog 8 (5), e1002721.

[2] Bunnik, E. M., Euler, Z., Welkers, M. R. A., Boeser-Nunnink, B. D. M., Grijsen, M. L., Prins, J. M., Schuitemaker, H., Aug. 2010. Adaptation of HIV-1 envelope gp120 to humoral immunity at a population level. Nat Med 16 (9), 991–993.

[3] Burton, D. R., Ahmed, R., Barouch, D. H., Butera, S. T., Crotty, S., Godzik, A., Kaufmann, D. E., McElrath, M. J., Nussenzweig, M. C., Pulendran, B., Scanlan, C. N., Schief, W. R., Silvestri, G., Streeck, H., Walker, B. D., Walker, L. M., Ward, A. B., Wilson, I. A., Wyatt, R., 2012. A Blueprint for HIV Vaccine Discovery. Cell Host Microbe 12 (4), 396–407.

[4] Burton, D. R., Poignard, P., Stanfield, R. L., Wilson, I. A., 2012. Broadly neutralizing antibodies present new prospects to counter highly antigenically diverse viruses. Science 337 (6091), 183–6.

[5] Burton, D. R., Stanfield, R. L., Wilson, I. A., 2005. Antibody vs. HIV in a clash of evolutionary titans. Proc Natl Acad Sci USA 102 (42), 14943–8.

[6] Cao, J., Sullivan, N., Desjardin, E., Parolin, C., Robinson, J., Wyatt, R., Sodroski, J., 1997. Replication and neutralization of human immunodeficiency virus type 1 lacking the V1 and V2 variable loops of the gp120 envelope glycoprotein. J Virol 71 (12), 9808–12.

[7] Chackerian, B., Rudensey, L., Overbaugh, J., OCT 1997. Specific N-linked and O-linked glycosylation modifications in the envelope V1 domain of simian immunodeficiency virus variants that evolve in the host alter recognition by neutralizing antibodies. J Virol 71 (10), 7719–7727.

[8] Chen, L., Kwon, Y. D., Zhou, T., Wu, X., O'Dell, S., Cavacini, L., Hessell, A. J., Pancera, M., Tang, M., Xu, L., Yang, Z. Y., Zhang, M. Y., Arthos, J., Burton, D. R., Dimitrov, D. S., Nabel, G. J., Posner, M. R., Sodroski, J., Wyatt, R., Mascola, J. R., Kwong, P. D., 2009. Structural basis of immune evasion at the site of CD4 attachment on HIV-1 gp120. Science 326 (5956), 1123–7.

[9] Chohan, B., Lang, D., Sagar, M., Korber, B., Lavreys, L., Richardson, B., Overbaugh, J., MAY 2005. Selection for human immunodeficiency virus type I envelope glycosylation variants with shorter V1-V2 loop sequences occurs during transmission of certain genetic subtypes and may impact viral RNA levels. J Virol 79 (10), 6528–6531.

[10] Curlin, M. E., Zioni, R., Hawes, S. E., Liu, Y., Deng, W., Gottlieb,

885 G. S., Zhu, T., Mullins, J. I., 2010. HIV-1 envelope subregion length
886 variation during disease progression. PLoS Pathog 6 (12), e1001228.

887 [11] Derdeyn, C. A., Decker, J. M., Bibollet-Ruche, F., Mokili, J. L., Mul-
888 doon, M., Denham, S. A., Heil, M. L., Kasolo, F., Musonda, R., Hahn,
889 B. H., Shaw, G. M., Korber, B. T., Allen, S., Hunter, E., 2004. Envelope-
890 constrained neutralization-sensitive HIV-1 after heterosexual transmis-
891 sion. Science 303 (5666), 2019–22.

892 [12] Doms, R. W., Earl, P. L., Chakrabarti, S., Moss, B., July 1990. Hu-
893 man immunodeficiency virus types 1 and 2 and simian immunodeficiency
894 virus env proteins possess a functionally conserved assembly domain. J
895 Virol 64 (7), 3537–3540.

896 [13] Doores, K. J., Burton, D. R., Oct. 2010. Variable Loop Glycan Depen-
897 dency of the Broad and Potent HIV-1-Neutralizing Antibodies PG9 and
898 PG16. Journal Of Virology 84 (20), 10510–10521.

899 [14] Doria-Rose, N. A., Georgiev, I., O'Dell, S., Chuang, G. Y., Staupe, R. P.,
900 McLellan, J. S., Gorman, J., Pancera, M., Bonsignori, M., Haynes, B. F.,
901 Burton, D. R., Koff, W. C., Kwong, P. D., Mascola, J. R., 2012. A Short
902 Segment of the HIV-1 gp120 V1/V2 Region Is a Major Determinant of
903 Resistance to V1/V2 Neutralizing Antibodies. J Virol 86 (15), 8319–23.

904 [15] Doria-Rose, N. A., Klein, R. M., Daniels, M. G., O'Dell, S., Nason, M.,
905 Lapedes, A., Bhattacharya, T., Migueles, S. A., Wyatt, R. T., Korber,
906 B. T., Mascola, J. R., Connors, M., 2010. Breadth of human immunod-

907 eficiency virus-specific neutralizing activity in sera: clustering analysis
908 and association with clinical variables. J Virol 84 (3), 1631–6.

909 [16] Fox, D., Balfe, P., Palmer, C., May, J., Arnold, C., McKeating, J.,
910 JAN 1997. Length polymorphism within the second variable region of
911 the human immunodeficiency virus type 1 envelope glycoprotein affects
912 accessibility of the receptor binding site. J Virol 71 (1), 759–765.

913 [17] Gallo, S. A., Finnegan, C. M., Viard, M., Raviv, Y., Dimitrov, A.,
914 Rawat, S. S., Puri, A., Durell, S., Blumenthal, R., 2003. The HIV Env-
915 mediated fusion reaction. Biochim Biophys Acta 1614 (1), 36–50.

916 [18] Goo, L., Milligan, C., Simonich, C. A., Nduati, R., Overbaugh, J., 2012.
917 Neutralizing Antibody Escape during HIV-1 Mother-to-Child Transmis-
918 sion Involves Conformational Masking of Distal Epitopes in Envelope.
919 J Virol 86 (18), 9566–82.

920 [19] Gorny, M. K., Stamatatos, L., Volsky, B., Revesz, K., Williams, C.,
921 Wang, X. H., Cohen, S., Staudinger, R., Zolla-Pazner, S., Mar. 2005.
922 Identification of a New Quaternary Neutralizing Epitope on Human Im-
923 munodeficiency Virus Type 1 Virus Particles. J Virol 79 (8), 5232–5237.

924 [20] Groenink, M., Fouchier, R. A., Broersen, S., Baker, C. H., Koot, M.,
925 van't Wout, A. B., Huisman, H. G., Miedema, F., Tersmette, M.,
926 Schuitemaker, H., 1993. Relation of phenotype evolution of HIV-1 to
927 envelope V2 configuration. Science 260 (5113), 1513–6.

928 [21] Harrington, P. R., Nelson, J. A. E., Kitrinos, K. M., Swanstrom, R.,
929 MAY 2007. Independent evolution of human immunodeficiency virus

type 1 env V1/V2 and V4/V5 hypervariable regions during chronic infection. J Virol 81 (10), 5413–5417.

[22] Herrera, C., Klasse, P. J., Kibler, C. W., Michael, E., Moore, J. P., Beddows, S., 2006. Dominant-negative effect of hetero-oligomerization on the function of the human immunodeficiency virus type 1 envelope glycoprotein complex. Virology 351 (1), 121–32.

[23] Hoxie, J. A., 2010. Toward an antibody-based HIV-1 vaccine. Annu Rev Med 61, 135–52.

[24] Hu, G., Liu, J., Taylor, K. A., Roux, K. H., 2011. Structural comparison of HIV-1 envelope spikes with and without the V1/V2 loop. J Virol 85 (6), 2741–50.

[25] Hughes, E. S., Bell, J. E., Simmonds, P., 1997. Investigation of population diversity of human immunodeficiency virus type 1 in vivo by nucleotide sequencing and length polymorphism analysis of the V1/V2 hypervariable region of env. J Gen Virol 78 (Pt 11), 2871–82.

[26] Johnson, W. E., Morgan, J., Reitter, J., Puffer, B. A., Czajak, S., Doms, R. W., Desrosiers, R. C., 2002. A replication-competent, neutralization-sensitive variant of simian immunodeficiency virus lacking 100 amino acids of envelope. J Virol 76 (5), 2075–86.

[27] Julien, J.-P., Lee, J. H., Cupo, A., Murin, C. D., Derking, R., Hoffenberg, S., Caulfield, M. J., King, C. R., Marozsan, A. J., Klasse, P. J., Sanders, R. W., Moore, J. P., Wilson, I. A., Ward, A. B., Feb. 2013.

Asymmetric recognition of the HIV-1 trimer by broadly neutralizing antibody PG9. Proceedings Of The National Academy Of Sciences Of The United States Of America.

[28] Klasse, P. J., 2007. Modeling how many envelope glycoprotein trimers per virion participate in human immunodeficiency virus infectivity and its neutralization by antibody. Virology 369 (2), 245–262.

[29] Klasse, P. J., Sattentau, Q. J., 2002. Occupancy and mechanism in antibody-mediated neutralization of animal viruses. J Gen Virol 83 (Pt 9), 2091–108.

[30] Koito, A., Harrowe, G., Levy, J. A., Cheng-Mayer, C., 1994. Functional role of the V1/V2 region of human immunodeficiency virus type 1 envelope glycoprotein gp120 in infection of primary macrophages and soluble CD4 neutralization. J Virol 68 (4), 2253–9.

[31] Kolchinsky, P., Kiprilov, E., Bartley, P., Rubinstein, R., Sodroski, J., 2001. Loss of a single N-linked glycan allows CD4-independent human immunodeficiency virus type 1 infection by altering the position of the gp120 V1/V2 variable loops. J Virol 75 (7), 3435–43.

[32] Krachmarov, C., Pinter, A., Honnen, W. J., Gorny, M. K., Nyambi, P. N., Zolla-Pazner, S., Kayman, S. C., 2005. Antibodies That Are Cross-Reactive for Human Immunodeficiency Virus Type 1 Clade A and Clade B V3 Domains Are Common in Patient Sera from Cameroon, but Their Neutralization Activity Is Usually Restricted by Epitope Masking. J Virol 79 (2), 780–90.

[33] Kwon, Y. D., Finzi, A., Wu, X., Dogo-Isonagie, C., Lee, L. K., Moore, L. R., Schmidt, S. D., Stuckey, J., Yang, Y., Zhou, T., Zhu, J., Vicic, D. A., Debnath, A. K., Shapiro, L., Bewley, C. A., Mascola, J. R., Sodroski, J. G., Kwong, P. D., 2012. Unliganded HIV-1 gp120 core structures assume the CD4-bound conformation with regulation by quaternary interactions and variable loops. Proc Natl Acad Sci USA.

[34] Kwong, P. D., Doyle, M. L., Casper, D. J., Cicala, C., Leavitt, S. A., Majeed, S., Steenbeke, T. D., Venturi, M., Chaiken, I., Fung, M., Katinger, H., Parren, P. W., Robinson, J., Van Ryk, D., Wang, L., Burton, D. R., Freire, E., Wyatt, R., Sodroski, J., Hendrickson, W. A., Arthos, J., 2002. HIV-1 evades antibody-mediated neutralization through conformational masking of receptor-binding sites. Nature 420 (6916), 678–82.

[35] Kwong, P. D., Mascola, J. R., 2012. Human Antibodies that Neutralize HIV-1: Identification, Structures, and B Cell Ontogenies. Immunity 37 (3), 412–25.

[36] Labrijn, A. F., Poignard, P., Raja, A., Zwick, M. B., Delgado, K., Franti, M., Binley, J., Vivona, V., Grundner, C., Huang, C. C., Venturi, M., Petropoulos, C. J., Wrin, T., Dimitrov, D. S., Robinson, J., Kwong, P. D., Wyatt, R. T., Sodroski, J., Burton, D. R., 2003. Access of antibody molecules to the conserved coreceptor binding site on glycoprotein gp120 is sterically restricted on primary human immunodeficiency virus type 1. J Virol 77 (19), 10557–65.

[37] Lamers, S. L., Sleasman, J. W., She, J. X., Barrie, K. A., Pomeroy, S. M., Barrett, D. J., Goodenow, M. M., 1993. Independent variation

and positive selection in env V1 and V2 domains within maternal-infant strains of human immunodeficiency virus type 1 in vivo. J Virol 67 (7), 3951–60.

[38] Li, Y., Cleveland, B., Klots, I., Travis, B., Richardson, B. A., Anderson, D., Montefiori, D., Polacino, P., Hu, S. L., 2008. Removal of a single N-linked glycan in human immunodeficiency virus type 1 gp120 results in an enhanced ability to induce neutralizing antibody responses. J Virol 82 (2), 638–51.

[39] Liu, J., Bartesaghi, A., Borgnia, M. J., Sapiro, G., Subramaniam, S., Jan 2008. Molecular architecture of native HIV-1 gp120 trimers. Nature 455 (7209), 109–U76.

[40] Liu, L., Cimbro, R., Lusso, P., Berger, E. A., Dec. 2011. Intraprotomer masking of third variable loop (V3) epitopes by the first and second variable loops (V1V2) within the native HIV-1 envelope glycoprotein trimer. Proc Natl Acad Sci USA 108 (50), 20148–20153.

[41] Losman, B., Bolmstedt, A., Schonning, K., Bjorndal, A., Westin, C., Fenyo, E. M., Olofsson, S., 2001. Protection of neutralization epitopes in the V3 loop of oligomeric human immunodeficiency virus type 1 glycoprotein 120 by N-linked oligosaccharides in the V1 region. AIDS Res Hum Retroviruses 17 (11), 1067–76.

[42] Ly, A., Stamatatos, L., 2000. V2 loop glycosylation of the human immunodeficiency virus type 1 SF162 envelope facilitates interaction of this protein with CD4 and CCR5 receptors and protects the virus from

neutralization by anti-V3 loop and anti-CD4 binding site antibodies. J Virol 74 (15), 6769–76.

[43] Magnus, C., Regoes, R. R., 2010. Estimating the stoichiometry of HIV neutralization. PLoS Comput Biol 6 (3), e1000713.

[44] Magnus, C., Regoes, R. R., 2012. Analysis of the Subunit Stoichiometries in Viral Entry. PLoS ONE 7 (3), e33441.

[45] Magnus, C., Rusert, P., Bonhoeffer, S., Trkola, A., Regoes, R. R., Feb 1 2009. Estimating the stoichiometry of human immunodeficiency virus entry. J Virol 83 (3), 1523–1531.

[46] Mao, Y., Wang, L., Gu, C., Herschhorn, A., Désormeaux, A., Finzi, A., Xiang, S.-H., Sodroski, J. G., 2013. Molecular architecture of the uncleaved HIV-1 envelope glycoprotein trimer. Proceedings Of The National Academy Of Sciences Of The United States Of America.

[47] Mao, Y., Wang, L., Gu, C., Herschhorn, A., Xiang, S. H., Haim, H., Yang, X., Sodroski, J., 2012. Subunit organization of the membrane-bound HIV-1 envelope glycoprotein trimer. Nat Struct Mol Biol.

[48] Mascola, J. R., Montefiori, D. C., 2010. The role of antibodies in HIV vaccines. Annu Rev Immunol 28, 413–44.

[49] McLellan, J. S., Pancera, M., Carrico, C., Gorman, J., Julien, J.-P., Khayat, R., Louder, R., Pejchal, R., Sastry, M., Dai, K., O'Dell, S., Patel, N., Shahzad-Ul-Hussan, S., Yang, Y., Zhang, B., Zhou, T., Zhu, J., Boyington, J. C., Chuang, G.-Y., Diwanji, D., Georgiev, I., Do Kwon,

Y., Lee, D., Louder, M. K., Moquin, S., Schmidt, S. D., Yang, Z.-Y., Bonsignori, M., Crump, J. A., Kapiga, S. H., Sam, N. E., Haynes, B. F., Burton, D. R., Koff, W. C., Walker, L. M., Phogat, S., Wyatt, R., Orwenyo, J., Wang, L.-X., Arthos, J., Bewley, C. A., Mascola, J. R., Nabel, G. J., Schief, W. R., Ward, A. B., Wilson, I. A., Kwong, P. D., Apr. 2011. Structure of HIV-1 gp120 V1/V2 domain with broadly neutralizing antibody PG9. Nature 480 (7377), 336–343.

[50] Montefiori, D. C. D., 2008. Measuring HIV neutralization in a luciferase reporter gene assay. Methods Mol Biol 485, 395–405.

[51] Morikita, T., Maeda, Y., Fujii, S., Matsushita, S., Obaru, K., Takatsuki, K., 1997. The V1/V2 region of human immunodeficiency virus type 1 modulates the sensitivity to neutralization by soluble CD4 and cellular tropism. AIDS Res Hum Retroviruses 13 (15), 1291–9.

[52] O'Rourke, S. M., Schweighardt, B., Phung, P., Fonseca, D. P., Terry, K., Wrin, T., Sinangil, F., Berman, P. W., 2010. Mutation at a single position in the V2 domain of the HIV-1 envelope protein confers neutralization sensitivity to a highly neutralization-resistant virus. J Virol 84 (21), 11200–9.

[53] Palmer, C., Balfe, P., Fox, D., May, J., Frederiksson, R., Fenyo, E., McKeating, J., JUN 15 1996. Functional characterization of the V1V2 region of human immunodeficiency virus type 1. Virology 220 (2), 436–449.

[54] Pastore, C., Nedellec, R., Ramos, A., Pontow, S., Ratner, L., Mosier,

1067 D. E., 2006. Human immunodeficiency virus type 1 coreceptor switch-
1068 ing: V1/V2 gain-of-fitness mutations compensate for V3 loss-of-fitness
1069 mutations. J Virol 80 (2), 750–8.

1070 [55] Pinter, A., Honnen, W. J., He, Y., Gorny, M. K., Zolla-Pazner, S., Kay-
1071 man, S. C., 2004. The V1/V2 domain of gp120 is a global regulator
1072 of the sensitivity of primary human immunodeficiency virus type 1 iso-
1073 lates to neutralization by antibodies commonly induced upon infection.
1074 J Virol 78 (10), 5205–15.

1075 [56] Quinones-Kochs, M. I., Buonocore, L., Rose, J. K., 2002. Role of N-
1076 linked glycans in a human immunodeficiency virus envelope glycopro-
1077 tein: effects on protein function and the neutralizing antibody response.
1078 J Virol 76 (9), 4199–211.

1079 [57] Ren, X., Sodroski, J., Yang, X., May 2005. An unrelated monoclonal
1080 antibody neutralizes human immunodeficiency virus type 1 by binding
1081 to an artificial epitope engineered in a functionally neutral region of the
1082 viral envelope glycoproteins. J Virol 79 (9), 5616–5624.

1083 [58] Ritola, K., Pilcher, C. D., Fiscus, S. A., Hoffman, N. G., Nelson, J. A.,
1084 Kitrinos, K. M., Hicks, C. B., Eron, J. J., J., Swanstrom, R., 2004. Mul-
1085 tiple V1/V2 env variants are frequently present during primary infection
1086 with human immunodeficiency virus type 1. J Virol 78 (20), 11208–18.

1087 [59] Robey, W., Safai, B., Oroszlan, S., Arthur, L., Gonda, M., Gallo,
1088 R., Fischinger, P., 1985. Characterization of envelope and core struc-

tural gene-products of HTLV-III with sera from AIDS patients. Science 228 (4699), 593–595.

[60] Robinson, J. E., Franco, K., Elliott, D. H., Maher, M. J., Reyna, A., Montefiori, D. C., Zolla-Pazner, S., Gorny, M. K., Kraft, Z., Stamatatos, L., 2010. Quaternary Epitope Specificities of Anti-HIV-1 Neutralizing Antibodies Generated in Rhesus Macaques Infected by the Simian/Human Immunodeficiency Virus SHIVSF162P4. J Virol 84 (7), 3443–53.

[61] Ross, T. M., Cullen, B. R., 1998. The ability of HIV type 1 to use CCR-3 as a coreceptor is controlled by envelope V1/V2 sequences acting in conjunction with a CCR-5 tropic V3 loop. Proc Natl Acad Sci USA 95 (13), 7682–6.

[62] Rusert, P., Krarup, A., Magnus, C., Brandenberg, O. F., Weber, J., Ehlert, A.-K., Regoes, R. R., Guenthard, H. F., Trkola, A., Jan 2011. Interaction of the gp120 V1V2 loop with a neighboring gp120 unit shields the HIV envelope trimer against cross-neutralizing antibodies. J Exp Med 208 (7), 1419–1433.

[63] Sagar, M., Wu, X., Lee, S., Overbaugh, J., OCT 2006. Human immunodeficiency virus type 1 V1-V2 envelope loop sequences expand and add glycosylation sites over the course of infection, and these modifications affect antibody neutralization sensitivity. J Virol 80 (19), 9586–9598.

[64] Salzwedel, K., Berger, E., Jan 2000. Cooperative subunit interactions within the oligomeric envelope glycoprotein of hiv-1: Functional com-

plementation of specific defects in gp120 and gp41. Proceedings of the National Academy of Science USA 97 (23), 12794–12799.

[65] Sattentau, Q. J., Moore, J. P., 1995. Human immunodeficiency virus type 1 neutralization is determined by epitope exposure on the gp120 oligomer. J Exp Med 182 (1), 185–96.

[66] Saunders, C. J., McCaffrey, R. A., Zharkikh, I., Kraft, Z., Malenbaum, S. E., Burke, B., Cheng-Mayer, C., Stamatatos, L., 2005. The V1, V2, and V3 regions of the human immunodeficiency virus type 1 envelope differentially affect the viral phenotype in an isolate-dependent manner. J Virol 79 (14), 9069–80.

[67] Schonning, K., Lund, O., Lund, O. S., Hansen, J.-E. S., 1999. Stoichiometry of monoclonal antibody neutralization of T-cell line-adapted human immunodeficiency virus type 1. J Virol, 8364–8370.

[68] Shibata, J., Yoshimura, K., Honda, A., Koito, A., Murakami, T., Matsushita, S., 2007. Impact of V2 mutations on escape from a potent neutralizing anti-V3 monoclonal antibody during in vitro selection of a primary human immunodeficiency virus type 1 isolate. J Virol 81 (8), 3757–68.

[69] Shioda, T., Levy, J. A., Cheng-Mayer, C., 1991. Macrophage and T cell-line tropisms of HIV-1 are determined by specific regions of the envelope gp120 gene. Nature 349 (6305), 167–9.

[70] Stamatatos, L., Cheng-Mayer, C., 1998. An envelope modification that renders a primary, neutralization-resistant clade B human immunodefi-

ciency virus type 1 isolate highly susceptible to neutralization by sera from other clades. J Virol 72 (10), 7840–5.

[71] Stamatatos, L., Morris, L., Burton, D. R., Mascola, J. R., 2009. Neutralizing antibodies generated during natural HIV-1 infection: good news for an HIV-1 vaccine? Nat Med 15 (8), 866–70.

[72] Stamatatos, L., Wiskerchen, M., Cheng-Mayer, C., 1998. Effect of major deletions in the V1 and V2 loops of a macrophage-tropic HIV type 1 isolate on viral envelope structure, cell entry, and replication. AIDS Res Hum Retroviruses 14 (13), 1129–39.

[73] Sullivan, N., Thali, M., Furman, C., Ho, D. D., Sodroski, J., 1993. Effect of amino acid changes in the V1/V2 region of the human immunodeficiency virus type 1 gp120 glycoprotein on subunit association, syncytium formation, and recognition by a neutralizing antibody. J Virol 67 (6), 3674–9.

[74] Toohey, K., Wehrly, K., Nishio, J., Perryman, S., Chesebro, B., 1995. Human immunodeficiency virus envelope V1 and V2 regions influence replication efficiency in macrophages by affecting virus spread. Virology 213 (1), 70–9.

[75] Veronese, F., Devico, A., Copeland, T., Oroszlan, S., Gallo, R., Sarngadharan, M., 1985. Characterization of gp41 as the transmembrane protein coded by the HTLV-III/LAV envelope gene. Science 229 (4720), 1402–1405.

[76] Walker, L., Phogat, S., Chan-Hui, P., Wagner, D., Phung, P., Goss, J., Wrin, T., Simek, M., Fling, S., Mitcham, J., Lehrman, J., Priddy, F., Olsen, O., Frey, S., Hammond, P., Kaminsky, S., Zamb, T., Moyle, M., Koff, W., Poignard, P., Burton, D., Jan 2009. Broad and Potent Neutralizing Antibodies from an African Donor Reveal a New HIV-1 Vaccine Target. Science 326 (5950), 285–289.

[77] Wei, X., Decker, J., Wang, S., Hui, H., Kappes, J., Wu, X., Salazar-Gonzalez, J., Salazar, M., Kilby, J., SAAG, M., Komarova, N., Nowak, M., HAHN, B., Kwong, P., SHAW, G., Jan 2003. Antibody neutralization and escape by HIV-1. Nature 422 (6929), 307–312.

[78] Wei, X., Decker, J. M., Liu, H., Zhang, Z., Arani, R. B., Kilby, J. M., Saag, M. S., Wu, X., Shaw, G. M., Kappes, J. C., 2002. Emergence of Resistant Human Immunodeficiency Virus Type 1 in Patients Receiving Fusion Inhibitor (T-20) Monotherapy. Antimicrob Agents Chemother, 1–10.

[79] White, T. A., Bartesaghi, A., Borgnia, M. J., Meyerson, J. R., de la Cruz, M. J. V., Bess, J. W., Nandwani, R., Hoxie, J. A., Lifson, J. D., Milne, J. L. S., Subramaniam, S., DEC 2010. Molecular Architectures of Trimeric SIV and HIV-1 Envelope Glycoproteins on Intact Viruses: Strain-Dependent Variation in Quaternary Structure. PLoS Pathog 6 (12).

[80] Wilen, C. B., Tilton, J. C., Doms, R. W., 2012. Molecular mechanisms of HIV entry. Adv Exp Med Biol 726, 223–42.

[81] Wolk, T., Schreiber, M., 2006. N-Glycans in the gp120 V1/V2 domain of the HIV-1 strain NL4-3 are indispensable for viral infectivity and resistance against antibody neutralization. Med Microbiol Immunol 195 (3), 165–72.

[82] Wu, X., Zhou, T., O'Dell, S., Wyatt, R. T., Kwong, P. D., Mascola, J. R., 2009. Mechanism of human immunodeficiency virus type 1 resistance to monoclonal antibody B12 that effectively targets the site of CD4 attachment. J Virol 83 (21), 10892–907.

[83] Wyatt, R., Moore, J., Accola, M., Desjardin, E., Robinson, J., Sodroski, J., 1995. Involvement of the V1/V2 variable loop structure in the exposure of human immunodeficiency virus type 1 gp120 epitopes induced by receptor binding. J Virol 69 (9), 5723–33.

[84] Wyatt, R., Sodroski, J., 1998. The HIV-1 envelope glycoproteins: fusogens, antigens, and immunogens. Science 280 (5371), 1884–1888.

[85] Wyatt, R., Sullivan, N., Thali, M., Repke, H., Ho, D., Robinson, J., Posner, M., Sodroski, J., 1993. Functional and immunologic characterization of human immunodeficiency virus type 1 envelope glycoproteins containing deletions of the major variable regions. J Virol 67 (8), 4557–65.

[86] Yang, X., Kurteva, S., Lee, S., Sodroski, J., 2005. Stoichiometry of antibody neutralization of Human Immunodeficiency Virus type 1. J Virol 79 (6), 3500–8.

[87] Yang, X., Kurteva, S., Ren, X., Lee, S., Sodroski, J., 2005. Stoichiometry of envelope glycoprotein trimers in the entry of Human Immunodeficiency Virus type 1. J Virol 79 (19), 12132–47.

[88] Yang, X., Kurteva, S., Ren, X., Lee, S., Sodroski, J., 2006. Subunit stoichiometry of human immunodeficiency virus type 1 envelope glycoprotein trimers during virus entry into host cells. J Virol 80 (9), 4388–95.

[89] Yang, X., Lipchina, I., Cocklin, S., Chaiken, I., Sodroski, J., November 2006. Antibody binding is a dominant determinant of the efficiency of human immunodeficiency virus type 1 neutralization. J Virol 80 (22), 11404–11408.

[90] Yang, Z. Y., Chakrabarti, B. K., Xu, L., Welcher, B., Kong, W. P., Leung, K., Panet, A., Mascola, J. R., Nabel, G. J., 2004. Selective modification of variable loops alters tropism and enhances immunogenicity of human immunodeficiency virus type 1 envelope. J Virol 78 (8), 4029–36.

[91] Zhu, P., Liu, J., Bess, Jr, J., Chertova, E., Lifson, J. D., Grise, H., Ofek, G. A., Taylor, K. A., Roux, K. H., 2006. Distribution and three-dimensional structure of AIDS virus envelope spikes. Nature 441 (7095), 847–52.

Figures

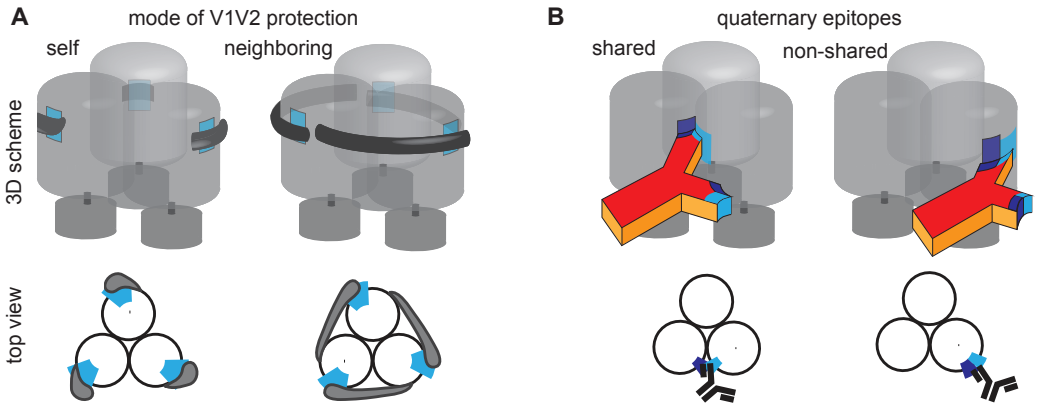

Figure 1: Sketch of the two main research questions addressed here. (A) Does the V1V2 loop protect V3 epitopes by shielding the epitope of the same protomer (self protection) or a neighboring protomer (neighboring protection)? (B) Does an antibody specific epitope consist of regions from different protomers (shared epitope) or from only one protomer (non-shared epitope)? The top row shows three-dimensional schematic representation of the envelope trimer with blue epitopes, dark grey V1V2 loops and red antibodies. The bottom row shows a two-dimensional scheme of the envelope protomers depicted as circles.

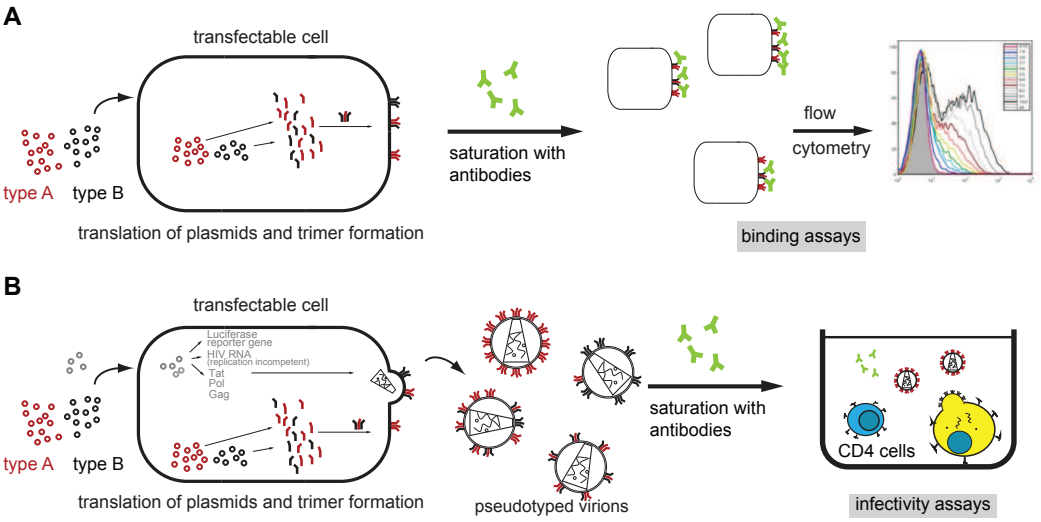

Figure 2: Sketch of the different experimental setups. **A** Transfection of virus producer cells with two types of plasmids encoding two different envelope protein types. The resulting trimer-expressing cells are saturated with fluorescently labeled antibodies and analyzed with flow cytometry. **B** To produce pseudotype virus stocks, cells are additionally transfected with plasmids encoding for the genetic information of the virion. The resulting pseudotype virions are saturated with antibodies and subjected to target cells, followed by scoring of target cell infection.

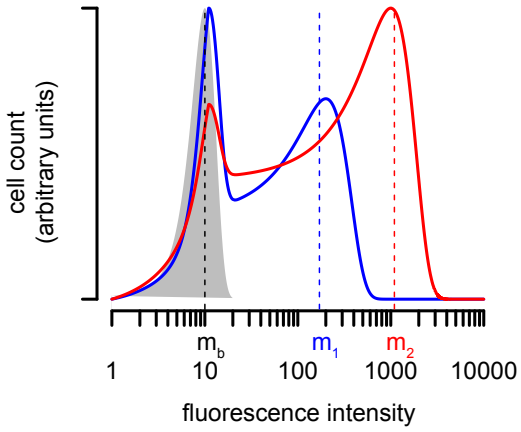

Figure 3: Schematic of a flow cytometry readout with three transfected cell populations. The grey shaded area represents the background signal of mock-transfected cells with mean fluorescence intensity m_b. The blue and the red curves are the fluorescence signals of two cell populations expressing different amounts of type 1 and type 2 envelope proteins with different sensitivities to a fluorescently labeled antibody against the epitope of interest. Their mean fluorescence intensity, MFI, can be calculated by subtracting the background mean fluorescence intensity, m_b from the mean of the whole curves m_1 and m_2, respectively. This means $\mathrm{MFI}_i = m_i - m_b$ for $i = 1, 2$. For the normalized mean fluorescence intensity, nMFI, the calculated mean fluorescence intensities have to be divided by the maximum of the mean fluorescence intensities, i.e. $\mathrm{nMFI_i} = (m_i - m_b)/\max\{\mathrm{MFI}_1, \mathrm{MFI}_2\}$.

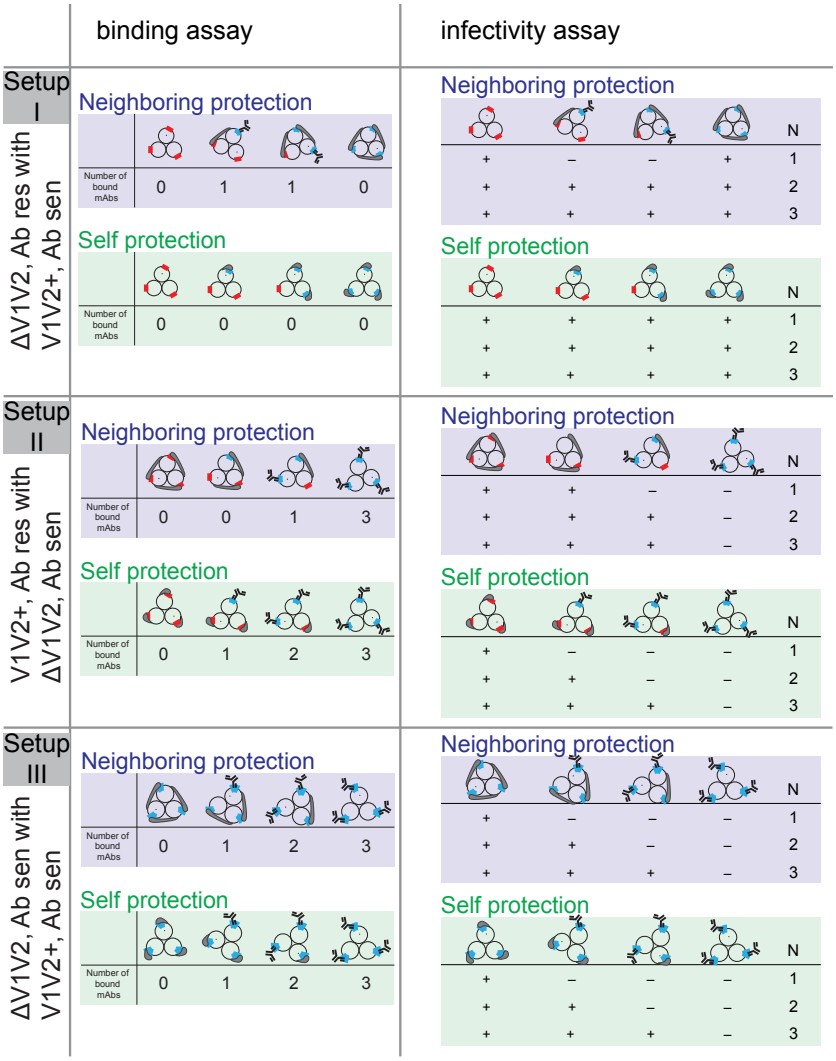

Figure 4: Trimer tables for differently mixed trimers (rows, referred to as setups) and testing experiments (columns, referred to as approaches) to study the mode of protection the V1V2 loop confers. Red rectangles represent antibody resistant binding sites and blue rectangles antibody sensitive sites. The grey shapes symbolize the V1V2 loops. In binding assays, the mean fluorescence intensity is a measure for the number of antibodies bound to an average trimer. Thus we show all envelope combinations and the number of antibodies bound in the two different protection modes. In infectivity assays, functional trimers (marked with a "+", non-functional trimers are marked with "–") take part in mediating cell entry. A trimer is functional if less than N antibodies are bound, as defined by the stoichiometry of trimer neutralization. Parts of this figure are adapted from figures 5, 6 and 7 in [62].

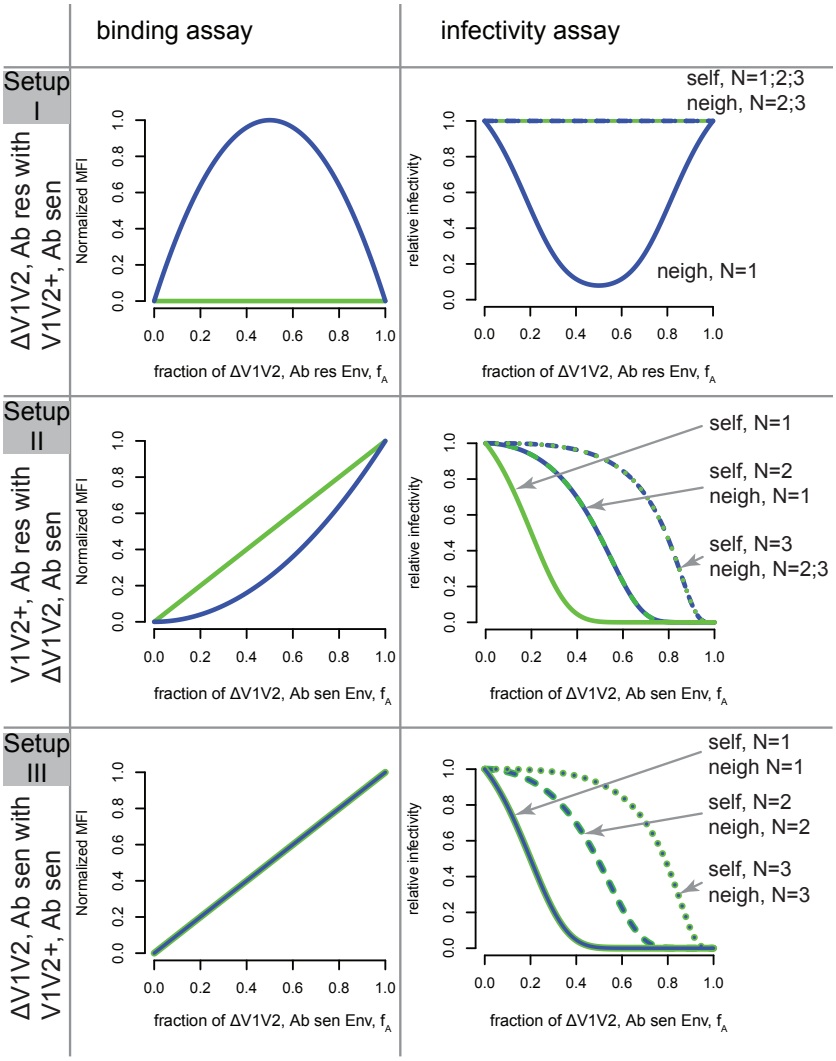

Figure 5: Predictions of our model for the mode of epitope masking by the V1V2 loop. This scheme contrasts the predictions of the normalized MFI measured in binding assays (left column) with the predictions of the relative infectivity in infectivity assays (right column) for all possible three envelope setups (rows). Predictions for the neighboring scenario are colored blue, predictions for the self protection scenario are colored green. Parts of this figure are adapted from figures 5 and 6 in [62].

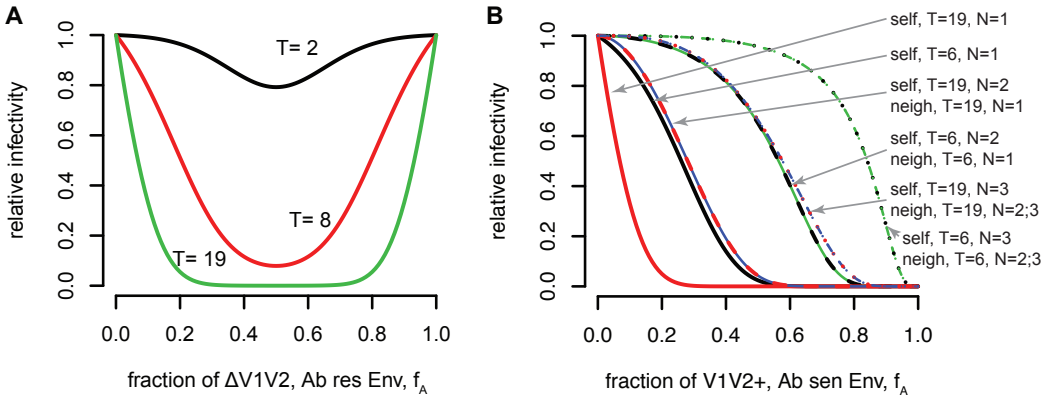

Figure 6: Influence of the stoichiometry of entry in infectivity experiments for **A** setup I and **B** setup II.

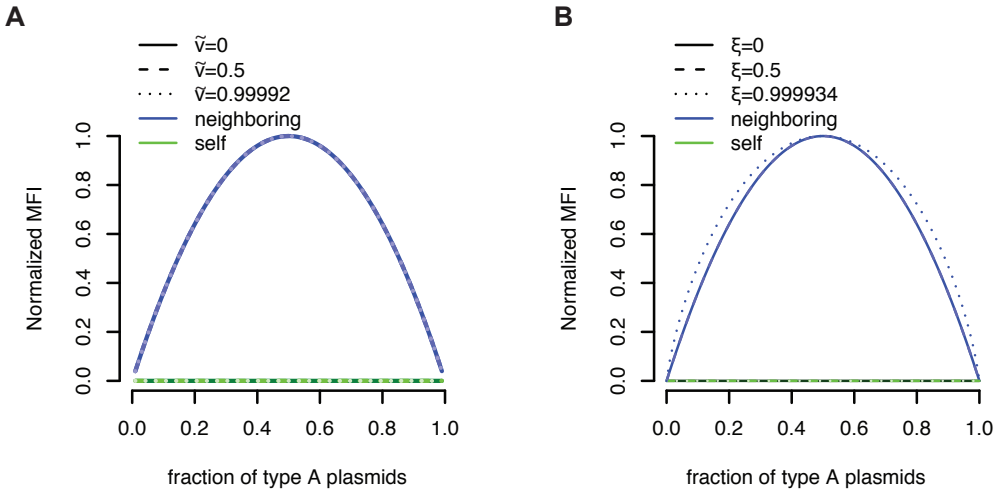

Figure 7: Influence of **A** imperfect transfection and **B** segregation on the predictions of the normalized mean fluorescence intensity for the experimental setup I in figure 4. Parts of this figure are adapted from figure S3 in [62].

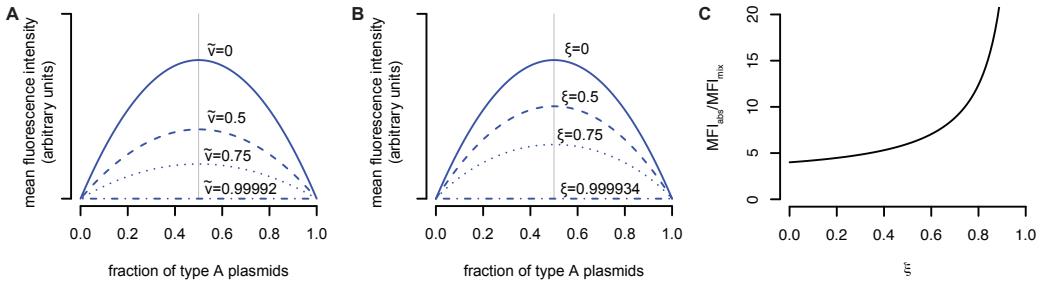

Figure 8: The influence of (A) imperfect transfection and (B) potential segregation on the mean fluorescence intensity for cell populations expressing mixed trimers of V1V2 deleted, antibody binding resistant envelope proteins with V1V2 expressing, antibody sensitive envelope proteins (setup I). As the signal in setup I comes from heterotrimers and as the fraction of heterotrimers decreases with increasing imperfect transfection ($\tilde{v} \to 1$) and segregation ($\xi \to 1$), the maximal value of the mean fluorescence intensity decreases. (C) The mean fluorescence intensity of a 100% antibody binding sensitive cell population, MFI_{abs} divided by the mean fluorescence intensity of a cell population transfected with equal amounts of envelope proteins of the two different types is a measure of how much the segregation parameter influences the expression of heterotrimers. The higher the segregation parameter is, the smaller is the mean fluorescence intensity of a cell population expressing mixed trimers.

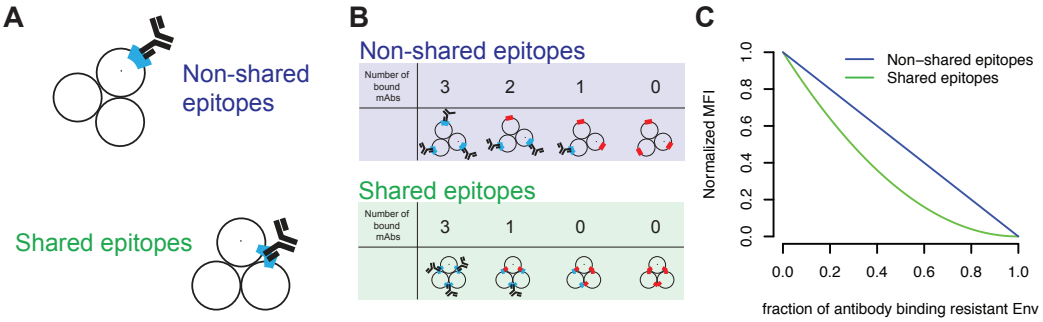

Figure 9: **A** Sketch of shared epitopes. The black circles represent one envelope protein. The epitope is marked blue. **B** Number of antibodies binding to the mixed trimers consisting of envelope proteins with intact epitopes (blue) or mutations making the envelope antibody binding resistant (red) for the two epitope scenarios shared (green shaded table) and non-shared (blue shaded table). **C** Theoretical predictions for the normalized mean fluorescence intensity.

Tables

Table 1: Parameter definitions.

f_i	fraction of type i envelope proteins in the envelope pool
RI	function for the relative infectivity
MFI	function for the mean fluorescence intensity
nMFI	function for the normalized mean fluorescence intensity
S	mode of protection (neighboring or self) or epitope (shared or non-shared)
T	stoichiometry of entry, number of trimer cell-receptor interactions required for infection
N	stoichiometry of neutralization, number of antibodies rendering one trimer non-functional
η_s	probability that virion has s trimers
$\alpha_{S,N}$	probability of forming a functional trimer
X	number of antibodies bound to one random trimer
$\mathbf{n}$	$= (n_0, n_1, n_2, n_3)$, vector with number of antibodies bound to trimers with 0,1,2,3 mutant envelope proteins
$\tilde{v}$	coefficient of variation
ξ	segregation coefficient

Table 2: Overview of the properties of the different assays using mixed trimers to resolve HIV envelope trimer functions.

	Binding assay	**Infectivity assay**
Mode of V1V2 protection: Distinction between inter- and intra-protomeric interaction	yes	only for some setups and stoichiometries, prior knowledge about stoichiometries necessary
Quaternary epitopes: Distinction between inter- and intra-protomeric interaction	yes	only for some setups and stoichiometries, prior knowledge about stoichiometries necessary
Determination of entry stoichiometry [28, 45, 87]	no	yes
Determination of stoichiometry of neutralization [28, 43, 86]	no	yes
Determination of subunit stoichiometries (CD4, coreceptor, fusion protein, subunit cooperation)[44, 88]	no	yes
Influenced by trimer segregation	yes	yes
Influenced by imperfect transfection	yes	yes
Influenced by trimer expression level on cell/virus surface	only the absolute fluorescence signal, but not the normalized mean fluorescence intensity	yes
Influenced by antibodies binding to monomer or dimer on cell/virus surface	yes	no
Influenced by antibodies binding to non-functional trimers	yes	no
Influenced by different infectivities/entry stoichiometries of homotrimers of the different envelope proteins used	no	yes